

2011

Design of Novel Pini Inhibitors Incorporating a p-Phospho-Glutamate Analogue

Jonathan Glen Meyer

Follow this and additional works at: <https://ir.lib.uwo.ca/digitizedtheses>

Recommended Citation

Meyer, Jonathan Glen, "Design of Novel Pini Inhibitors Incorporating a p-Phospho-Glutamate Analogue" (2011). *Digitized Theses*. 3304.

<https://ir.lib.uwo.ca/digitizedtheses/3304>

This Thesis is brought to you for free and open access by the Digitized Special Collections at Scholarship@Western. It has been accepted for inclusion in Digitized Theses by an authorized administrator of Scholarship@Western. For more information, please contact wlsadmin@uwo.ca.

**Design of Novel Pin1 Inhibitors Incorporating a β -Phospho-Glutamate
Analogue**

**(Spine Title: Novel Pin1 Inhibitors Incorporating a β -Phos-Glutamate
Analogue)**

(Thesis Format: Integrated article)

by

Jonathan Glen Meyer

2

Graduate Program in Biochemistry

**A thesis submitted in partial fulfillment
of the requirements for the degree of
Master of Science**

School of Graduate and Postdoctoral Studies

The University of Western Ontario

London, Ontario, Canada

THE UNIVERSITY OF WESTERN ONTARIO
SCHOOL OF GRADUATE AND POSTDOCTORAL STUDIES

CERTIFICATE OF EXAMINATION

Supervisor

Dr. Gilles Lajoie

Supervisory Committee

Dr. Rob Hudson

Dr. Brian Shilton

Examiners

Dr. Rob Hudson

Dr. James Choy

Dr. Gary Shaw

The thesis by

Jonathan Glen Meyer

Entitled:

**Design of Novel Pin1 Inhibitors Incorporating a β -Phospho-Glutamate
Analogue**

Is accepted in partial fulfillment of the
requirements for the degree of
Master of Science

Date _____

Chair of the Thesis Examination Board

Abstract

Pin1 is an enzyme essential to cell cycle regulation and has a key role in cancer proliferation. This thesis reports ongoing efforts to obtain a Pin1 inhibitor exhibiting an inhibition constant in the nanomolar range.

It was previously found that Pin1 activity could be inhibited using a short proline containing peptide sequence which also contains a stereospecific β -substituted α -amino acid. Several proline analogues were tested for greater inhibition against Pin1 than previously synthesized Cbz-L-Glu(β -phos)-Pro-NH₂. It was found that using full length Pin1 in the chymotrypsin-coupled photometric assay rendered different values than using only the catalytic PPlase domain for Cbz-L-Glu(β -phos)-Pro-NH₂, $K_i = 54.1 \pm 1.8 \mu\text{M}$ and $20 \pm 0.9 \mu\text{M}$ respectively. The potential effectiveness of the synthesized inhibitors against Pin1 was assessed using the same convenient chymotrypsin-coupled photometric assay against full length Pin1.

This thesis describes the synthesis of two novel compounds which exhibited an increase in inhibition relative to Cbz-L-Glu(β -phos)-Pro-NH₂ ($K_i = 54.1 \pm 1.8 \mu\text{M}$) with results in the micromolar range; Cbz-L-Glu(β -phos)-Pip-NH₂ ($K_i = 45.4 \pm 1.1 \mu\text{M}$) and Cbz-L-Glu(β -phos)-Methylpiperazine ($K_i = 22.7 \pm 1.4 \mu\text{M}$).

Keywords: Pin1, OBO ester, Pin1 inhibition, β -substituted glutamic acid, chymotrypsin coupled kinetic assay.

Faint, illegible text at the top of the page, possibly a title or introductory paragraph.

Second paragraph of faint, illegible text.

To my wife Alyssa

Third paragraph of faint, illegible text.

Fourth paragraph of faint, illegible text.

Acknowledgements

First and foremost I would like to thank Dr. Gilles Lajoie for your depth of knowledge, encouragement, and patience. I would also like to thank the members my advisory committee Dr. Brian Shilton and Dr. Robert Hudson for your advice and guidance.

Sincere gratitude goes to Paula Pittock, Chris Hughes, and Yinyin Laio for all the technical assistance, idea bouncing and moral support. Also, I had the pleasure of working with the greatest research group and I would like to thank each one for contributing to my work: Dustin George, Amelia Nuhn, Suya Liu, Zheng Ye, Sean Bendall, Larry Campbell, and Jennifer Ballard.

I would like to thank Alister Gould from the Shilton lab for training me on the photospectrometer and allowing me to work into his schedule.

Finally I would like to thank Alyssa and all of my friends and family for their continuing support and encouragement; I most definitely would not have been able to do it without you.

Table of Contents

| | |
|------------------------------------|-----|
| Abstract | iii |
| Dedication | iv |
| Acknowledgements | v |
| Table of Contents | vi |
| List of Tables | ix |
| List of Schemes | ix |
| List of Figures | x |
| List of Abbreviations | xii |

Chapter One: Introduction

| | |
|--|----|
| 1.1 Peptidyl-Prolyl <i>cis-trans</i> Isomerase (PPIase) Activity | 1 |
| 1.2 Pin1 | 3 |
| 1.2.1 Structure, Domains, and Recognition Motif of Pin1 | 3 |
| 1.2.2 Pin1 PPIase Mechanism | 5 |
| 1.2.3 Pin1 Interaction Partners and Disease States | 6 |
| 1.3 Pin1 in Cell Cycle Regulation and Cancer | 6 |
| 1.4 Pin1 and Alzheimer's Disease | 7 |
| 1.5 HIV | 8 |
| 1.6 Pin1 Inhibition | 9 |
| 1.7 Stereoselective Synthesis of β -substituted Serine Analogues | 12 |
| 1.8 Stereoselective Addition to Carbonyl Groups | 15 |
| 1.9 Liquid Phase Peptide Synthesis | 17 |

| | |
|--|----|
| 1.10 Solid Phase Peptide Synthesis | 18 |
| 1.11 Phosphorylation of Synthesized Peptides | 19 |
| 1.12 Chymotrypsin Coupled Kinetic Assay | 21 |
| 1.13 Thesis Overview | 23 |
| Chapter One References | 26 |

Chapter Two: Results & Discussion

| | |
|--|----|
| 2.1 Synthesis of N, C Protected Serine Aldehyde..... | 30 |
| 2.2 Reformatsky Addition..... | 32 |
| 2.3 Synthesis of Cbz-Glu(t-butyl)(β -OH)-OH..... | 41 |
| 2.4 Selection of Pin1 Inhibitor Analogues | 43 |
| 2.5 Synthesis of Pin1 Inhibitors..... | 44 |
| 2.5.1 Solid Phase Preparation | 44 |
| 2.5.1.1 Synthesis of Cbz-Glu(β -phos)-Pip-NH ₂ | 44 |
| 2.5.1.2 Attempted Synthesis of Cbz-Glu(β -phos)-Pip-NAL-NH ₂ | 44 |
| 2.5.2 Liquid Phase Preparation..... | 45 |
| 2.6 Pin1 Inhibitor Activity..... | 49 |
| Chapter Two References | 60 |

Chapter Three: Experimental

| | |
|------------------------------|----|
| 3.1 Instrumentation | 62 |
| 3.2 Reagents | 63 |
| 3.3 Chemical Synthesis | 64 |

| | |
|--|----|
| 3.3.1 Oxetane Tosylate, 1 | 64 |
| 3.3.2 Cbz- <i>L</i> -Ser-Oxetane Ester, 2..... | 64 |
| 3.3.3 Cbz- <i>L</i> -Ser-OBO Ester, 3 | 65 |
| 3.3.4 Cbz- <i>L</i> -Ser(ald)-OBO Ester, 4 | 66 |
| 3.3.5 Cbz- <i>L</i> -Glu(OtBu)(β -OH)-OBO Ester, 5..... | 67 |
| 3.3.6 Cbz- <i>L</i> -Glu(OtBu)(β -OH)-OH, 6..... | 68 |
| 3.3.7 General Liquid Phase Peptide Coupling and Phosphorylation..... | 69 |
| 3.3.8 General Protocol for Cleavage of Protecting Groups | 70 |
| 3.3.9 Solid Phase Peptide Synthesis | 70 |
| 3.3.10 Resin Cleavage and Protecting Group Removal..... | 71 |
| 3.3.11 Chymotrypsin Coupled Kinetic Assay | 72 |
| Chapter Three References | 73 |

Chapter Four: Conclusion

| | |
|------------------------|----|
| 4.1 Conclusion | 74 |
| 4.2 Future Work | 75 |
| Curriculum Vitae | 77 |

List of Tables

| | |
|--|----|
| Table 1.1 | 10 |
| Peptide sequences of select peptide inhibitors. | |
| Table 2.1 | 38 |
| Summary of methods attempted. The * denotes trials which were performed with additional washing steps. | |
| Table 2.2 | 53 |
| Summary of Pin1 inhibition assays. | |
| Table 3.1 | 71 |
| Summary results of peptides synthesized. | |

List of Schemes

| | |
|-------------------------|----|
| Scheme 1.1 | 14 |
| Scheme 1.2 | 19 |
| Scheme 1.3 | 21 |
| Scheme 2.1 | 31 |
| Scheme 2.2 | 42 |
| Scheme 2.3 | 47 |

List of Figures

| | |
|---|----|
| Figure 1.1 | 2 |
| Visual representation of A) non-proline containing peptide bond in <i>trans</i> and <i>cis</i> conformations and B) proline containing peptide bond in <i>trans</i> and <i>cis</i> conformations. | |
| Figure 1.2 | 5 |
| The PPlase domain, denoted by hollow arrows, are in approximately the same orientation to demonstrate the high degree of freedom of movement of the WW domain, denoted by solid arrows. A) Crystal structure, pdb code 2ZQS, of Pin1 mutant C113A [31] B) NMR structure, pdb code 1NMV, of Pin1 [32]. | |
| Figure 1.3 | 11 |
| Selection of Pin1 inhibitors. | |
| Figure 1.4 | 12 |
| Structural representation of Cbz-Glu(β -phos)-Pro-NH ₂ | |
| Figure 1.5 | 15 |
| Major product prediction using Cram's rule. Where L is a large substituent, M is a medium sized substituent and S is a small substituent such as hydrogen. | |
| Figure 1.6 | 16 |
| Major product prediction using the Felkin-Anh model. Where L is a large substituent, M is a medium sized substituent and S is a small substituent such as hydrogen. | |
| Figure 1.7 | 17 |
| Major product prediction using 1,2 chelation controlled addition. Where L is a large substituent and S is a small substituent such as hydrogen. | |
| Figure 1.8 | 22 |
| Schematic representation of the chymotrypsin coupled kinetic assay developed by Fischer <i>et al.</i> [58] | |
| Figure 1.9 | 22 |
| A) Peptide substrate suc-AEPF-pNA in the non-cleavable <i>cis</i> conformation and B) peptide substrate suc-AEPF-pNA in the cleavable <i>trans</i> conformation | |
| Figure 2.1 | 35 |
| 400 MHz ¹ H NMR of Cbz-L-Ser-OBO, 3 . | |
| Figure 2.2 | 36 |
| 400 MHz ¹ H NMR of Cbz-L-Ser(ald)-OBO, 4 . | |

List of Abbreviations

Figure 2.3 41
Newman projections showing addition to Cbz-Ser(ald)-OBO using A) Cram's rule, B) most probable addition using the Felkin-Anh model, C/D) possible conformations of addition using a 1,2 chelation control mechanism E) Newman projection of the major product formed, **5**. Where R is the Cbz protecting group.

Figure 2.4 48
Visualization of electron delocalization in aniline.

Figure 2.5 51
Sample raw data of chymotrypsin coupled Pin1 enzymatic assays. A) Representation of assay without inhibitor present. B) Assay in presence of an inhibitor. i) represents time point where chymotrypsin is added; ii) represents time point where Pin1 is added; iii) represents the tangent line of the background chemical conversion rate; iv) represents the tangent line of the initial rate of Pin1 isomerization.

Figure 2.6 54
Pin1 inhibition Michaelis-Menten plot of synthesized inhibitors which demonstrated inhibition activity (n=1).

Figure 2.7 56
NMR structure of the binding pocket of Pin1. Bound to Pin1 is the peptide Ac-Phe-D-Thr(PO₃)-Pip-NAL-Gln-NH₂ (Thr(PO₃)-Pip-NAL-Gln shown) adapted from Zheng *et al.* [8].

Figure 2.8 59
Structural representations of PiB and PiJ

List of Abbreviations

| | |
|------------------------------------|---|
| Abs | Absorbance |
| Ac ₂ O | Acetic anhydride |
| APP | Amyloid Precursor Protein |
| A3G | APOBEC3G |
| Aβ ₄₂ | Amyloid Beta peptide 42 |
| BF ₃ ·Et ₂ O | Boron trifluoride diethyl etherate |
| BOC | t-Butyloxycarbonyl |
| Bth | 3-Benzothienylalanine |
| ca. | Circa (approximately) |
| Calcd | Calculated |
| Cbz | Benzyloxycarbonyl |
| CsA | Cyclosporin A |
| Cyp | Cyclophilin |
| <i>D</i> | <i>dextro</i> |
| DIPEA | N, N-Diisopropylethylamine |
| DMF | N, N-Dimethylformamide |
| DMSO | Dimethyl sulfoxide |
| <i>E. coli</i> | <i>Escherichia coli</i> |
| Equ | Equivalence |
| ESI-MS | Electrospray Ionization Mass Spectrometry |
| Et ₂ O | Diethyl ether |

| | |
|-------------------|---|
| EtOH | Ethanol |
| Et ₃ N | Triethylamine |
| EtMgBr | Ethyl magnesium bromide |
| EtOAc | Ethyl acetate |
| FKBPs | FK506 binding proteins |
| Fmoc | 9-fluorenylmethyloxycarbonyl |
| g | Gram |
| h | Hour |
| HBTU | 2-(1H-Benzotriazole-1-yl)-1,1,3,3-tetramethyluronium- hexafluorophosphate |
| HCl | Hydrochloric acid |
| HF | Hydrofluoric acid |
| HIV | Human Immunodeficiency Virus |
| HOBT | 1-hydroxy-benzotriazole |
| K _i | Inhibition constant |
| L | <i>levo</i> |
| L | Litre |
| LPPS | Liquid Phase Peptide Synthesis |
| M | Molar |
| mCPBA | <i>meta</i> -chloroperoxybenzoic acid |
| MeOH | Methanol |
| mg | Milligram |
| MHPD | 2-methyl-2 hydroxymethyl-1,3-propanediol |
| min | Minute |

| | |
|--------|--|
| mL | Milliliter |
| mM | Millimolar |
| mmol | Millimole |
| mol | Mole |
| MP | Melting point |
| MS | Mass spectrometry |
| NAL | Naphthylalanine |
| NIMA | <u>N</u> ever in <u>M</u> itosis gene <u>A</u> |
| nM | Nanomolar |
| NMR | Nuclear magnetic resonance |
| OBO | 4-methyl-2, 6, 7-trioxabicyclo[2.2.2]octane |
| Oxe-Ts | Oxetane tosylate |
| PAL | 5-(4-Fmoc-aminomethyl-3,5-dimethoxyphenoxy)-valeric acid-MBHA |
| Ph | Phenyl |
| pH | Measure of concentration of Hydrogen or Hydroxide ions in solution |
| Pin1 | <u>P</u> eptidylprolyl <i>cis/trans</i> <u>I</u> somerase, <u>N</u> IMA-interacting <u>1</u> |
| pip | Pipecolic acid |
| pNA | Para-nitroaniline |
| PPIase | Peptidyl-prolyl <i>cis-trans</i> isomerase |
| PPiC | <u>P</u> eptidyl-prolyl <i>cis-trans</i> <u>I</u> somerase <u>C</u> |
| ppm | Parts per million |
| Pro | Proline |
| R | <i>rectus</i> |

| | |
|---------------|--------------------------------|
| RBF | Round bottomed flask |
| RNAP2 | Ribonucleic acid polymerase 2 |
| <i>re</i> | <i>rectus</i> |
| <i>S</i> | <i>sinister</i> |
| s | Second |
| Ser | Serine |
| <i>si</i> | <i>sinister</i> |
| SPPS | Solid phase peptide synthesis |
| tbba | tertiary-butyl bromoacetate |
| TEA | Triethylamine |
| Thr | Threonine |
| t-butyl | Tertiary-butyl |
| TFA | Trifluoroacetic acid |
| THF | Tetrahydrofuran |
| TIPS | Triisopropylsilane |
| TLC | Thin layer chromatography |
| TsCl | Para-toluenesulphonyl chloride |
| UV | Ultraviolet |
| VIS | Visible |
| α | alpha |
| β | beta |
| λ | lambda, wavelength |
| μL | Microlitre |

μm micrometer

μM Micromolar

π pi

σ sigma

ω omega

% Percent

$^{\circ}$ Degrees

$^{\circ}\text{C}$ Degrees Celsius

Chapter One: Introduction

1.1 Peptidyl-Prolyl *cis-trans* Isomerase (PPIase) Activity

Proteins are a sequence of amino acids linked together in series through amide or peptide, bonds. Due to the partial double bond properties in the amide bond there are two conformations available in each peptide bond called *cis* and *trans*. *Cis* and *trans* can be defined as the dihedral angle, ω , between neighbouring α -carbons with an angle of 180° for *trans* and 0° for *cis* (see Figure 1.1). The *trans* conformation of a peptide bond is favoured over the *cis* conformation in nearly all naturally occurring peptide bonds. This is due to increased conformational strain experienced in the *cis* conformation through steric hindrance. The steric hindrance experienced is between neighbouring α -carbon substituents, both the residue side chain as well as the carbonyl group. However, in a proline containing peptide bond, where proline is on the nitrogen side of the bond, both the *cis* and *trans* conformations are closer in terms of steric hindrance due to the higher substitution on the amide nitrogen (Figure 1.1). With the higher substitution on the nitrogen, the propensity for the *trans* isomer is reduced from 1000:1, in a non-proline containing peptide bond, to approximately 3:1, with proline on the nitrogen side of the peptide bond. Thus, both isomers are naturally found in biological conditions.

Peptidyl-prolyl *cis-trans* isomerase (PPIase) activity catalyzes the relatively slow *cis-trans* isomerization of the prolyl-amide bond. PPIase activity affects protein regulation, folding, and biological activity of many target proteins

[1-4]. PPLase activity is ubiquitously found in both prokaryotic and eukaryotic organisms. There are three families of proteins which possess PPLase activity; the FK506 binding proteins (FKBPs), the cyclophilins (CyPs), and the parvulin family of proteins.

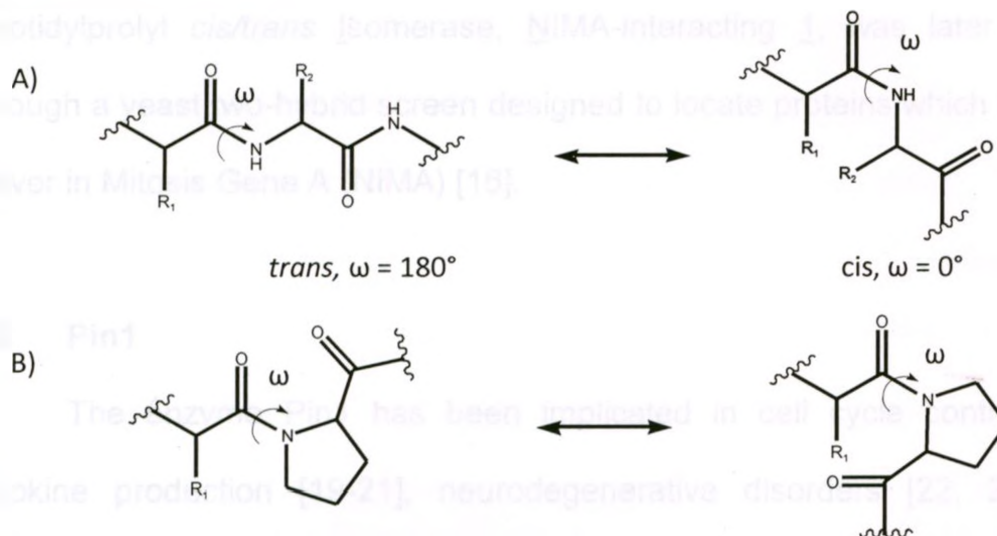


Figure 1.1 Visual representation of A) non-proline containing peptide bond in *trans* and *cis* conformations and B) proline containing peptide bond in *trans* and *cis* conformations.

The CyPs and FKBPs, which are also known as immunophilins, possess immunosuppressant activity [5] and bind to the immunosuppressant drugs cyclosporin A (CsA) and FK506 respectively, from which they derive their names [6]. However, the PPLase functionality of the immunophilins is not necessary for their immunosuppressive effects. It is the topology of the protein-drug complex which affects immunosuppressant activity. Upon binding to the respective immunosuppressant drug, the topology of the protein changes which then interferes with the transduction pathway blocking T-cell activation [2, 6]. CyPs and FKBPs have been shown to influence the folding of several proteins such as

collagen [7-9], carbonic anhydrase [10, 11], chymotrypsin inhibitor [12], and ribonuclease [13]. However, there is no definitive evidence that the PPlase activity of both the CyPs and FKBP is essential *in vivo*.

PPiC (peptidyl-prolyl *cis-trans* isomerase), isolated from *E. coli*, was the first of the parvulin family to be categorized [14, 15]. The human homologue Pin1, Peptidylprolyl *cis/trans* Isomerase, NIMA-interacting 1, was later discovered through a yeast two-hybrid screen designed to locate proteins which interact with Never in Mitosis Gene A (NIMA) [16].

1.2 Pin1

The enzyme Pin1 has been implicated in cell cycle control [17, 18], cytokine production [19-21], neurodegenerative disorders [22, 23], Human Immunodeficiency Virus (HIV) proliferation [24], and tumourgenesis [25] making it an attractive target for research.

1.2.1 Structure, Domains, and Recognition Motif of Pin1

Whereas Pin4/Par14 found in mice, consists only of a PPlase domain, Human Pin1 is composed of two domains, the tryptophan rich WW domain on the N-terminus (residues 1-39) and the C-terminal catalytic PPlase domain (residues 45-163) [16, 26].

The WW domain binds to proline rich or proline containing regions of proteins/peptides [27]. The WW domain of Pin1 is classified as a Group IV protein-protein interaction domain which binds to pSer/pThr proline ligands [27].

The small domain is an anti-parallel β -sheet consisting of three strands connected in series with short loop regions. Interestingly, the WW domain family is the smallest protein domain classified that does not require any ligands, disulphide bonds, or cofactors to remain stable [28]. Furthermore, the WW domain has been shown to act as a recruiting domain, allowing interaction partners to bind as well as bring substrates close to enzymes [29].

The larger PPlase domain also interacts with proline containing sequences, specifically with ligands containing pSer/pThr-proline. The PPlase domain consists of a β -sheet of four strands arranged in an anti-parallel fashion forming a beta roll in the center of the domain, one 3/10 helix, and three α -helices. Helices 1-3 (α -helix 1 and 2 as well as the 3/10 helix) are arranged around the central sheet on the convex side of the roll. However, helix 4 (α -helix 3) is arranged on the concave side of the roll effectively closing the gap on one side of the roll. The active site on the domain is located on the open side of the roll. The PPlase domain is highly conserved in the parvulin family among most species [30].

Currently there is conflicting evidence on the overall structural arrangement of the protein domains. NMR data suggests that the WW domain and the PPlase domain remain loosely arranged, whereas crystal structure data promotes close interaction between the WW and PPlase domains [31, 32]. Figure 1.2 depicts both NMR and crystal structures of Pin1.

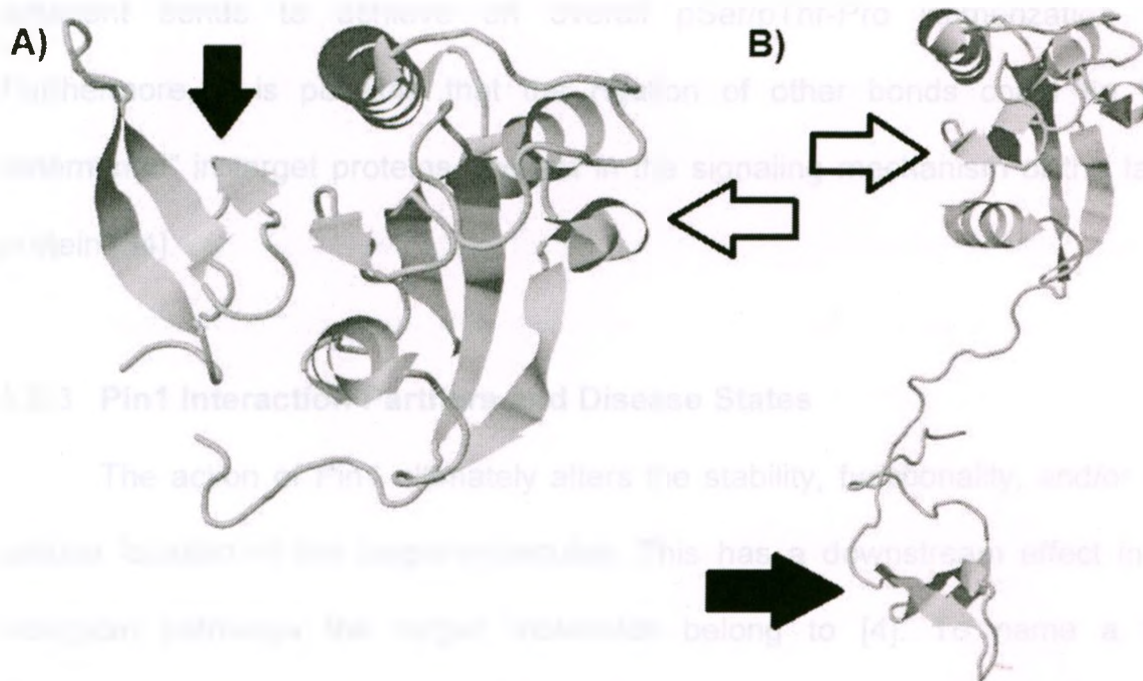


Figure 1.2 The PPlase domain, denoted by hollow arrows, are in approximately the same orientation to demonstrate the high degree of freedom of movement of the WW domain, denoted by solid arrows. A) Crystal structure, pdb code 2ZQS, of Pin1 mutant C113A [31] B) NMR structure, pdb code 1NMV, of Pin1 [32].

1.2.2 Pin1 PPlase Mechanism

The mechanism of Pin1 activity is not fully understood, however, it is known that Pin1 does not make or break a bond [33]. The rotation of solely the prolyl-amide bond, while maintaining the conformation of all other bonds, is considered a highly unfavourable mechanism. For the rotation of only the prolyl-amide bond a large shift in the ligand's structure would have to occur. This would require a large amount of free energy in the transition state. This mechanism of action may be possible for smaller peptide structures; however, this could lead to an unfavourable loss of binding energy in the complex. The rotation of the prolyl

peptide bond could also be accomplished by the rotation of several other adjacent bonds to achieve an overall pSer/pThr-Pro isomerization [34]. Furthermore, it is possible that the rotation of other bonds could be “pre-determined” in target proteins and act in the signaling mechanism of the target protein [34].

1.2.3 Pin1 Interaction Partners and Disease States

The action of Pin1 ultimately alters the stability, functionality, and/or final cellular location of the target molecules. This has a downstream effect in the biological pathways the target molecules belong to [4]. To name a few, interactions with NIMA [16], Cyclin D1 [18], Cdc25 phosphatase [35], phosphorylated Myt1 [35], PLK1 [36], p73 [37], p53 [38], phosphorylated tau protein [39, 40], and CK2 [41] have been identified for Pin1. All of these Pin1 interactions occur in a phosphorylation dependant manner [4, 40, 42]. Pin1 has also been shown to interact with transcription factors such as RNA Polymerase II (RNAP2) [4]. Clearly, Pin1 has an important role in cell regulation and function.

1.3 Pin1 in Cell Cycle Regulation and Cancer

NIMA is a mitotic kinase in *Asperillus nidulans* where overexpression induces premature chromosome condensation followed by apoptosis. However, if Pin1 is also overexpressed there is a prevention of the premature chromosome condensation. It was also shown that the overexpression of just Pin1 leads to the inhibition of transition into mitosis causing G2 arrest [16]. In this case G2 arrest is

caused by the inactivation of cell division cycle 2 (CDC2) and Cyclin B [42]. Low Pin1 levels have been shown to cause an increase in abnormal G2 to M transitions [17]. In this regard, Pin1 could potentially act as a molecular timer for the cell cycle.

However, Pin1 has been found to be up-regulated in several cancers including prostate, ovarian, and breast [43]. It is possible that up-regulation or overexpression of Pin1 can lead to uncontrolled abhorrent cell proliferation causing cancer.

Thus, there is evidence that Pin1 acts as a protector against oncogenic transformations, as well as has a tumourigenic effect. It is clear that Pin1 has a complex involvement in cell cycle regulation.

1.4 Pin1 and Alzheimer's Disease

Pin1 has been shown to regulate the phosphorylated state of both Tau and amyloid precursor protein (APP) through *cis/trans* isomerization [23, 40]. Loss of Pin1 function has shown an age dependent relationship for Tau and related pathologies in mice. It has also been revealed that neural tissue of Alzheimer's disease patients have a significantly lower amount of functional Pin1 [39]. In the absence of Pin1, A β 42 is formed which leads to plaque formation whereas in the presence of Pin1 the supposedly benign α -APP is formed [40]. Thus, it can be concluded that Pin1 acts to guard neural tissue from plaque formation.

Interestingly, it was shown through a longitudinal study that there is an inverse correlation between Alzheimer's disease and cancer in patients [44]. The development of one disease seems to inhibit the development of the other. Pin1 expression and activity has been implicated in these findings.

1.5 HIV

The human cytosine deaminase APOBEC3G (A3G) restricts the incorporation and replication of Human Immunodeficiency Virus (HIV) virions in human cells [45]. *In vivo* assays indicate that cells containing a reduced activity Pin1 mutant and wild type A3G have stronger resistance to HIV. However, cells with wild type Pin1 and wild type A3G have a higher incorporation rate of HIV [24]. Cells containing no A3G were found to have the highest infection rate. Thus, it can be concluded that Pin1 activity is influential in HIV infection rate. The study also concluded that wild type Pin1 has a strong interaction with A3G, while the W34A Pin1 mutant has minimal interaction with A3G, providing evidence that the interaction is not non-specific.

Interestingly, HIV-1 contains the genetic code for an accessory protein, Vif, which is thought to increase the phosphorylation at Ser16 on Pin1. Pin1 is not overexpressed in Vif mediated phosphorylation control but it would appear that the activity of pSer16 Pin1 has been increased [24]. The mechanism for the increased phosphorylation state and the increased activity is currently not well understood.

1.6 Pin1 Inhibition

As mentioned, Pin1 has an intricate and not fully understood role in several different cellular functions. The ability for researchers to control the function of Pin1 could lead to break-through developments in cancer, Alzheimer's disease, and potentially HIV research. Research into Pin1 inhibition began with the discovery that juglone, 5-hydroxy-1,4-naphthalenedione, derived from the black walnut (*Juglans nigra*) tree, was an irreversible inhibitor of Pin1 [46]. Unfortunately, juglone has been shown to be too toxic, making it a poor pharmaceutical agent [47].

The majority of the synthetic inhibitors for Pin1 are peptide sequences which contain a proline analogue such as pipercolic acid (pip) [48-51] and/or other hydrophobic, non-proteinaceous amino acids, such as naphthylalanine (NAL) [50, 51] and 3-benzothienyl alanine (Bth) [50], many with K_i values in the nM- μ M range. These peptide chain style of inhibitors contain residues which are not part of the recognition sequence of Pin1. The residues outside the binding picket are free to interact with accessory binding pockets on the proteins surface near the active site, thus increasing affinity. Table 1.1 demonstrates the sequences of a select few peptide chain inhibitors.

Ac-Ala-Ala-(D)-Ser(PO₃H₂)-Pro-Leu-pNA IC₅₀ = 1.0 μM [52]
 Ac-Ala-Ala-(D)-Ser(PO₃H₂)-Pro-Arg-pNA IC₅₀ = 3.6 μM [52]
 Ac-Ala-Ala-(D)-Ser-Pro-Leu-pNA IC₅₀ = 85 μM [52]
 cyclo(Arg-Arg-Arg-D-pThr-Pip-Nal-Arg-Arg-Gln) IC₅₀ = 1.1 μM [53]
 cyclo(D-Ala-Ile-D-pSer-Pro-Nal-Orn-Gln) IC₅₀ = 1.1 μM [53]
 cyclo(D-Arg-D-Arg-D-pThr-Pip-Nal-Arg-Gln) IC₅₀ = 0.22 μM [53]
 cyclo(Cys-Arg-Tyr-Pro-Glu-Val-Glu-Ile-Cys) K_i = 0.5 μM [54]
 Ac-Phe-D-Thr(PO₃H₂)-Pip-Nal-Gln-NH₂ K_i = 20.4 nM [51]
 Ac-Bth-Thr(PO₃H₂)-Pip-Nal-Gln-NH₂ K_i = 258 nM [50]
 Ac-Lys(*N*-biotinoyl)-Ala-Ala-Phe-D-Thr(PO₃H₂)-Pip-Nal-Gln-NH₂ K_i = 4.8 nM [50]

Table 1.1 Peptide sequences of select peptide inhibitors.

Other compounds have also been designed as potential Pin1 inhibitors. Different experimental approaches have been attempted such as testing different ring structures [48], creating conformationally locked substrate mimics [55], and synthesizing juglone-like molecules [56]. Figure 1.3 shows a selection of Pin1 inhibitors and their respective inhibition constants.

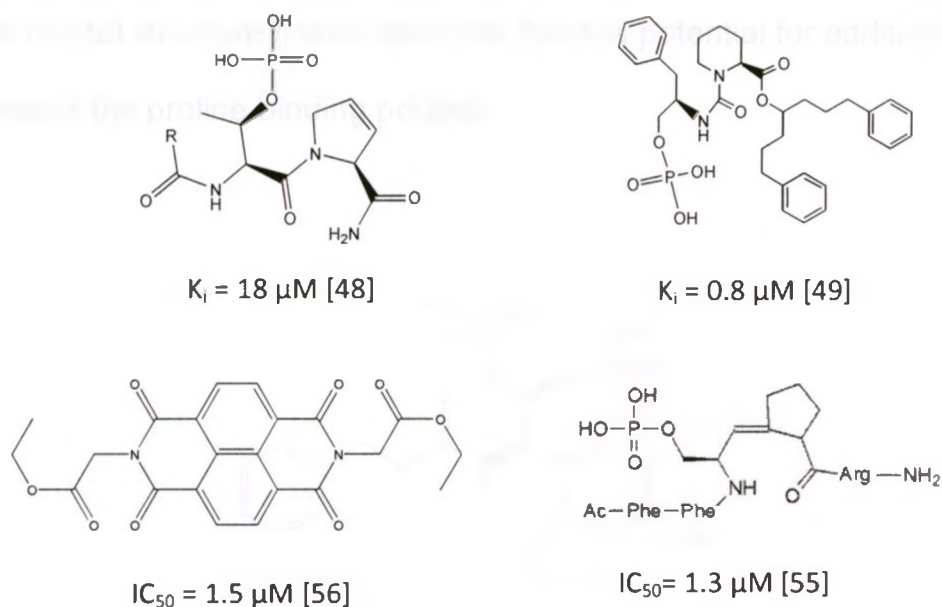


Figure 1.3 Selection of Pin1 inhibitors.

An attempt to increase the inhibiting potential of the dipeptide pSer-Pro was explored previously by Laio and Lajoie (unpublished) through addition to the serine β -carbon. Laio and Lajoie tested the effectiveness of different diastereomeric configurations of non-proteinaceous substitutions of ethyl, phenyl and acetyl groups on the serine β -carbon. The substitutions were then evaluated for Pin1 inhibition. The addition of an acetyl group in the **2S**, **3R** configuration, Cbz-Glu(β -phos)-Pro-NH₂ (Figure 1.4), proved to have the best inhibiting ability ($K_i = 20.0 \pm 0.9 \mu\text{M}$). From these studies it was postulated that the β -carboxy group binds to the arginine on the surface of Pin1. This is based on modeling the inhibitor with the crystal structure complex bound to a peptide inhibitor [51]. Using

the same crystal structure it was seen that there is potential for additional binding in and around the proline binding pocket.

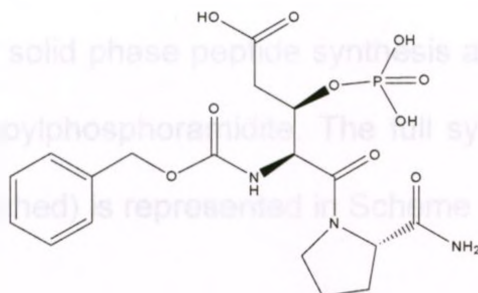


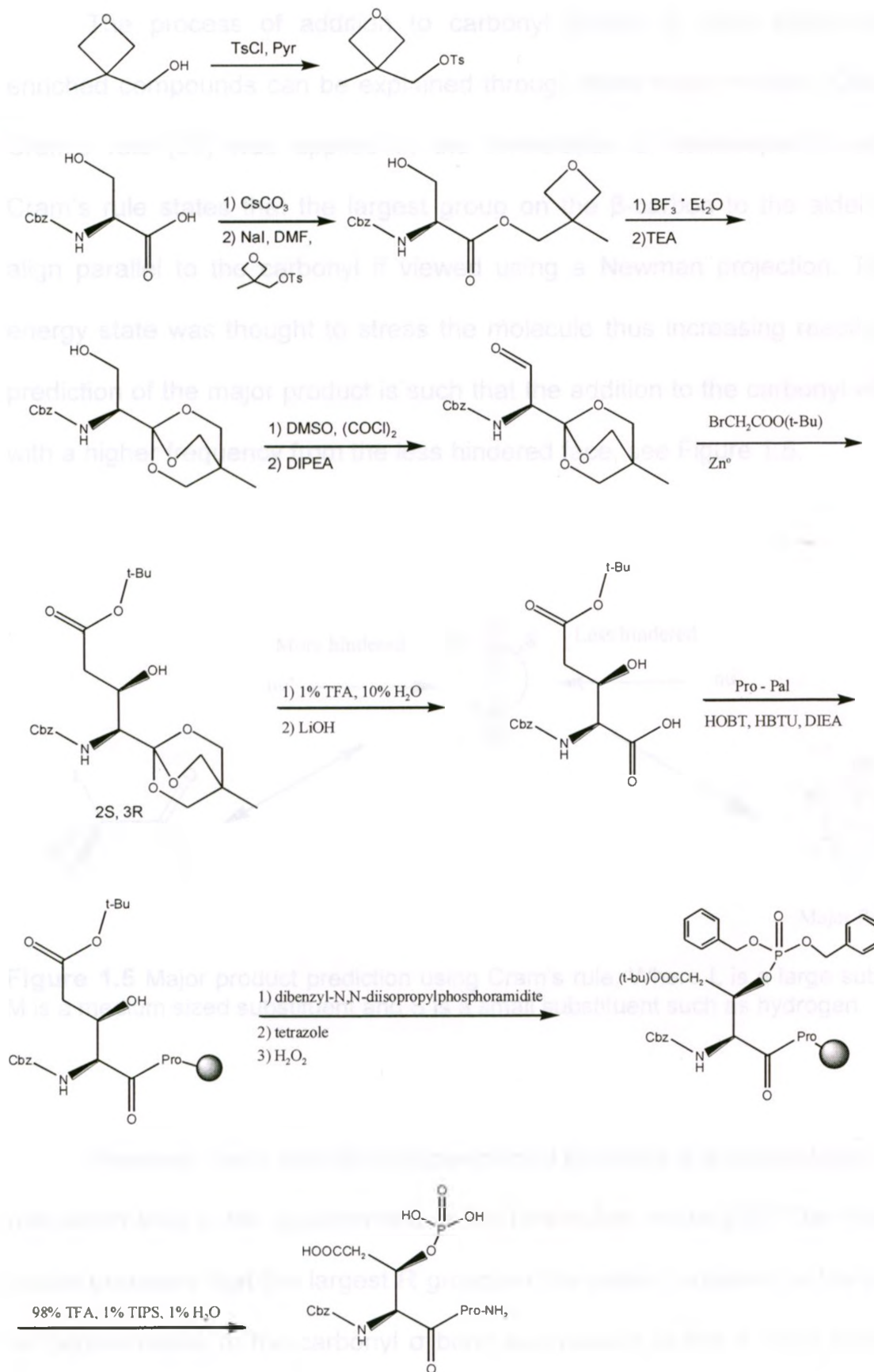
Figure 1.4 Structural representation of Cbz-Glu(β -phos)-Pro-NH₂

1.7 Stereoselective Synthesis of β -substituted Serine Analogues

A unique method for synthesis a of β -aldehyde serine analogue was developed by Blaskovich and Lajoie in 1993 [57] and a full synthesis of Cbz-Glu(β -phos)-Pro-NH₂ using the β -aldehyde strategy was completed by Laio and Lajoie in 2008 (unpublished). The method utilizes the 4-methyl-2,6,7-trioxabicyclo[2.2.2]octane ester (OBO ester) to retain the functionality of the carboxylic acid, to protect the chirality at the α -carbon as, well as to direct the addition at the β -carbonyl. The orthoester is added to Cbz N-protected serine through the esterification, and subsequent rearrangement, of oxetane to the carboxylic acid. The OBO ester significantly reduces the acidity of the α -proton which in turn reduces the propensity of enolization in the presence of the β -aldehyde, thus helping to maintain the chiral integrity of the α -carbon. The bulky

OBO ester also has the ability to direct stereoselective addition to the β -aldehyde in subsequent reactions. To synthesize Cbz-Glu(β -phos)-Pro-NH₂, the Reformatsky addition was used to add a t-butyl protected acetate group to the β -carbon. The OBO ester was selectively removed and the resulting free acid was coupled to proline using solid phase peptide synthesis and phosphorylated using dibenzyl- N, N- diisopropylphosphoramidite. The full synthetic strategy used by Laio and Lajoie (unpublished) is represented in Scheme 1.1.

1.8 Stereoselective Addition **Scheme 1.1**



1.8 Stereoselective Addition to Carbonyl Groups

The process of addition to carbonyl groups to form enantiomerically enriched compounds can be explained through three major models. Classically, Cram's rule [58] was applied in the formulation of stereospecific additions. Cram's rule states that the largest group on the β -carbon to the aldehyde will align parallel to the carbonyl if viewed using a Newman projection. This high energy state was thought to stress the molecule thus increasing reactivity. The prediction of the major product is such that the addition to the carbonyl will occur with a higher frequency from the less hindered face, see Figure 1.5.

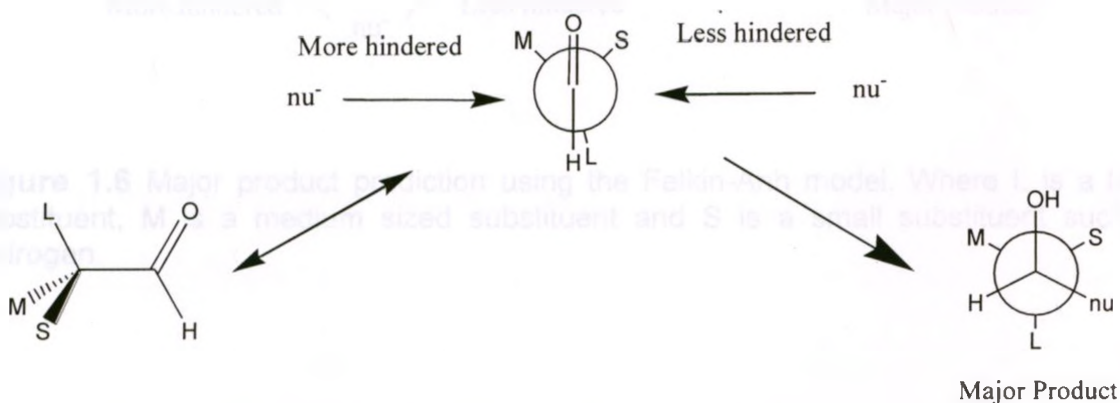


Figure 1.5 Major product prediction using Cram's rule. Where L is a large substituent, M is a medium sized substituent and S is a small substituent such as hydrogen.

However, there was some experimental evidence that contradicted Cram's rule which led to the development of the Felkin-Anh model [59]. The Felkin-Anh model proposes that the largest R group on the carbon adjacent to the carbonyl be perpendicular to the carbonyl σ bond and parallel to the π bond orbital. The

Bürgi-Dunitz angle of attack would need to be satisfied for addition, and thus the least hindered attacking angle is the preferred addition face (Figure 1.6).

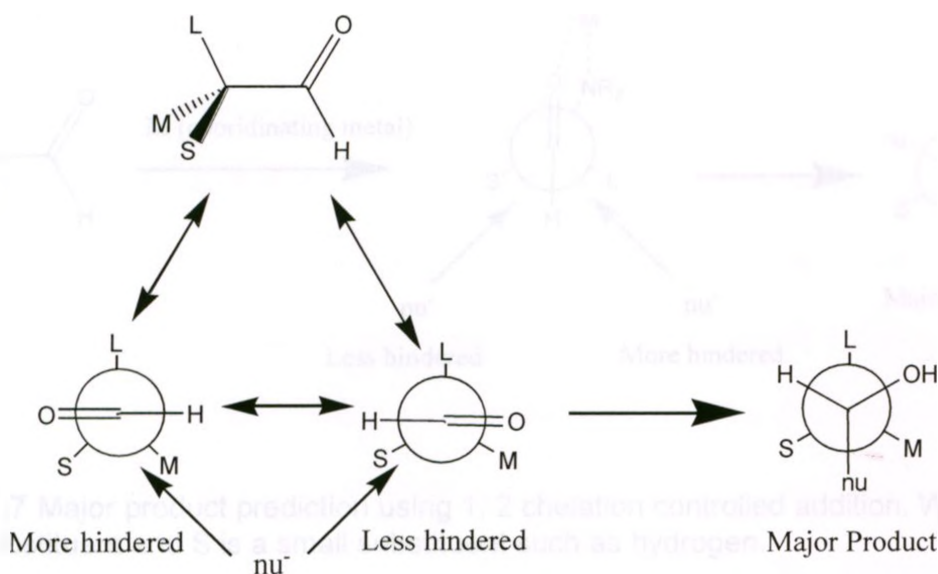


Figure 1.6 Major product prediction using the Felkin-Anh model. Where L is a large substituent, M is a medium sized substituent and S is a small substituent such as hydrogen.

An alternative way to predict the addition to a carbonyl group is through chelation control. A soluble coordinating metal ion, such as Zn^{2+} , is able to coordinate with the carbonyl and adjacent functional groups which are electron rich. Depending on the existing configuration of the molecule the coordinating ion will "hold" a target molecule in position to expose either the *re* or *si* face to the nucleophile. The major product from 1, 2 or 1, 3 chelation control is completely

dependent on the existing stereochemistry, the existence of an electron donor group, and the use of a coordinating metal ion (Figure 1.7)

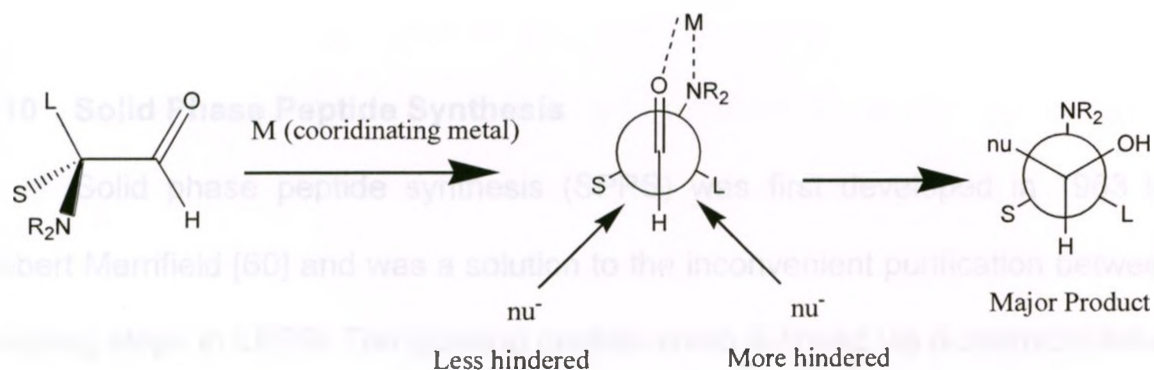


Figure 1.7 Major product prediction using 1, 2 chelation controlled addition. Where L is a large substituent and S is a small substituent such as hydrogen.

The Felkin-Anh model and Cram's rule do not always render the same major product. The use of a less coordinating metal will reduce the effects of chelation control in species which do poses electron rich centers. Using these three models, chemical reactions can be optimized to produce a product in high enantiomer excess.

1.9 Liquid Phase Peptide Synthesis

Liquid phase peptide synthesis (LPPS) is the original approach to peptide synthesis. The growing peptide chain is assembled through a lengthy series of coupling and purification steps. Some major drawbacks of LPPS are the difficult

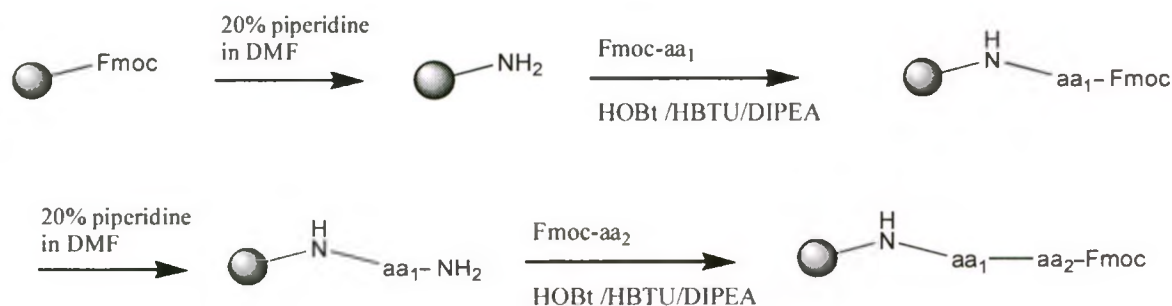
purification of the intermediate products and the length of time required for the synthesis. A major development in peptide synthesis removed the difficult purification by synthesizing peptide chains on insoluble resins.

1.10 Solid Phase Peptide Synthesis

Solid phase peptide synthesis (SPPS) was first developed in 1963 by Robert Merrifield [60] and was a solution to the inconvenient purification between coupling steps in LPPS. The growing peptide chain is linked via a chemical linker to an insoluble solid support resin. The resin can be rinsed between coupling steps, removing all unwanted elements of the synthesis, without the concern for loss of product. Synthesis of the peptide proceeds in the C-terminal to N-terminal direction through the use of protected amino acids. There are two main strategies available for SPPS: Boc and Fmoc. Both strategies use orthogonal cleavage steps, where the N-terminus protecting group can be removed without cleaving the resin-peptide linkage or the functional group protectors. In t-butyloxycarbonyl (Boc) chemistry the Boc N-protected residues are deprotected by neat trifluoroacetic acid (TFA) and the side chain protecting groups and the resin linker/peptide bond can be cleaved using concentrated HF. 9-fluorenylmethyloxycarbonyl (Fmoc) is removed using 20% piperidine in DMF and TFA removes the peptide from the resin and cleaves off the side chain protective groups. Due to the use of extremely hazardous HF in the BOC strategy, Fmoc chemistry is now generally preferred. Each residue addition cycle requires a

deprotection of the N-protected group on the growing chain and addition of a N-protected residue using hydroxybenzotriazole (HOBT), 2-(1H-benzotriazole-1-yl)-1,1,3,3-tetramethyluronium hexafluorophosphate (HBTU) and diisopropylethylamine (DIPEA). The type of resin linker used determines the properties of the cleaved product. For example, using PAL resin (5-(4-Fmoc-aminomethyl-3,5-dimethoxyphenoxy)-valeric acid-MBHA) as the solid support leaves the peptide C-terminal end amidated upon cleavage, whereas using Wang resin renders the C-terminal as a free carboxylic acid. Scheme 1.2 demonstrates a general synthesis of a dipeptide using an Fmoc protected PAL resin.

Scheme 1.2

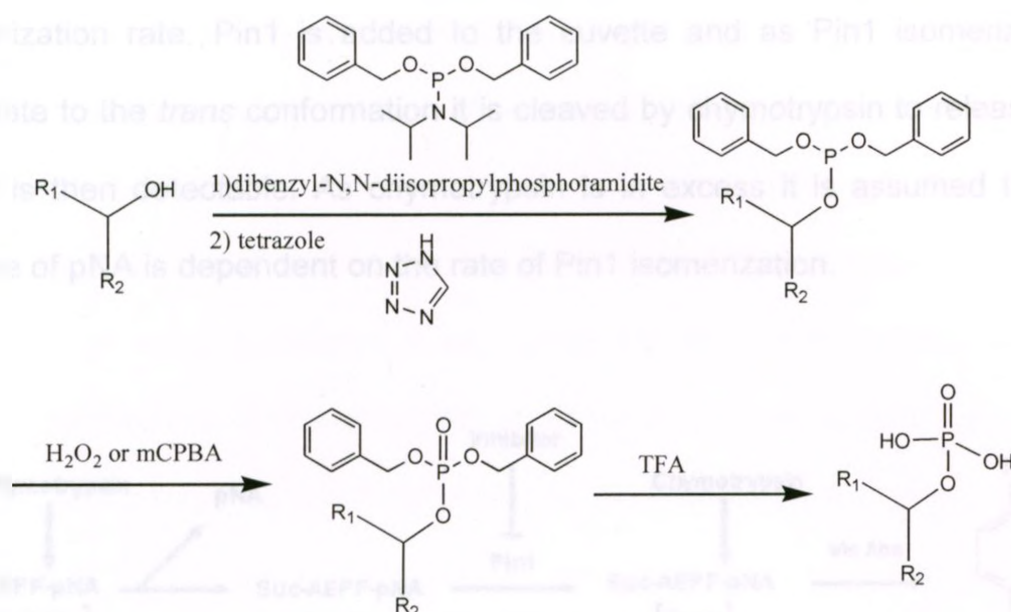


1.11 Phosphorylation of Synthesized Peptides

In peptide synthesis there are two phosphorylation strategies available: 1) using protected, phosphorylated amino acids as a building block during the peptide synthesis and 2) the "global phosphorylation" method where all free

unprotected hydroxyls available are phosphorylated upon completion of the peptide. Global phosphorylation requires the use of unprotected hydroxyl groups on the residues which are intended to be phosphorylated. Global phosphorylation is generally carried out using phosphoramidite class reagents such as N-diisopropylphosphoramidite or N-dibenzoylphosphoramidite in the presence of tetrazole to add phosphite ether to free hydroxyls. This is subsequently oxidized to a phosphotriester using H_2O_2 or mCPBA. The phosphate protecting groups can then be removed using a strong acid such as TFA, which is convenient for Fmoc SPPS as TFA will also cleave the protecting groups from other residues, as well decouple the synthesized peptide from the solid support. Scheme 1.3 depicts a general global phosphorylation of a hydroxyl using dibenzyl- N, N-diisopropylphosphoramidite.

Scheme 1.3



1.12 Chymotrypsin Coupled Kinetic Assay

Inhibitors can be assayed using a convenient photometric assay developed by Fischer *et al.* [61], see Figure 1.8. Chymotrypsin hydrolyses the phenylalanine-pNA amide linkage of the substrate suc-AEPF-pNA. This action releases free pNA into solution which is then detectable by UV/VIS absorption. The assay relies on the selectivity of chymotrypsin; chymotrypsin will only cleave the pNA from the substrate peptide when the E-P bond of the substrate is in the *trans* conformation (Figure 1.9).

After the initial burst phase of hydrolysis, the assay is allowed to proceed to ensure that all remaining substrate in solution is in the *cis* conformation. However, there is a small amount of peptide that is converted to the *trans*

conformation thermally in solution. This background chemical conversion rate must be subtracted from the observed isomerization rate to give the Pin1 isomerization rate. Pin1 is added to the cuvette and as Pin1 isomerizes the substrate to the *trans* conformation it is cleaved by chymotrypsin to release pNA which is then detectable. As chymotrypsin is in excess it is assumed that the release of pNA is dependent on the rate of Pin1 isomerization.

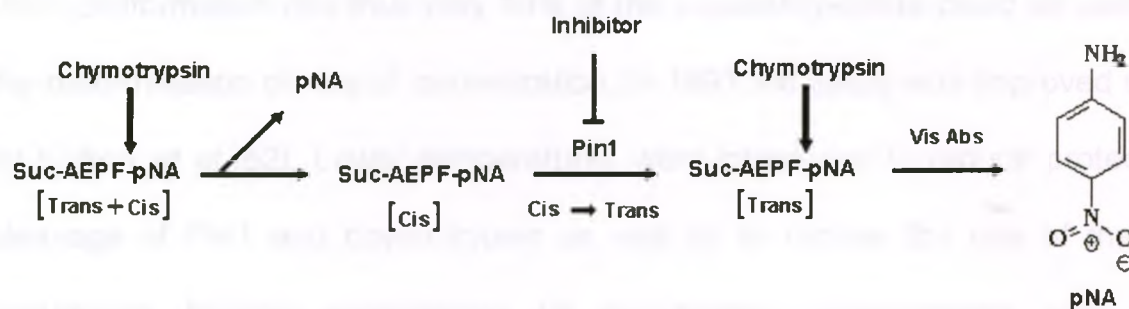


Figure 1.8 Schematic representation of the chymotrypsin coupled kinetic assay developed by Fischer *et al.* [58]

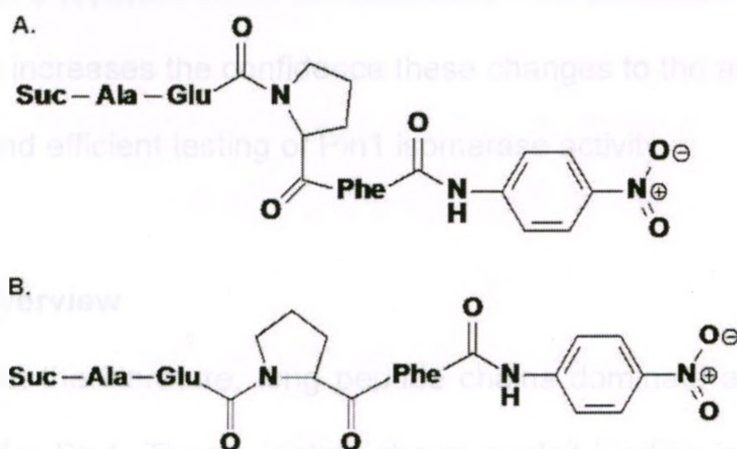


Figure 1.9 A) peptide substrate suc-AEPF-pNA in the non-cleavable *cis* conformation and B) peptide substrate suc-AEPF-pNA in the cleavable *trans* conformation

To determine the effectiveness of the inhibitors, the different inhibitors are added to the assay cuvette along with the substrate. Curves generated in the presence of inhibitor are compared to those generated in the absence of an inhibitor. Though the concentration of substrate varies with each individual trial, the concentration of Pin1 and the inhibitor remain constant throughout all trials.

The initial amount of substrate in the *cis* conformation is a major drawback of the assay. In aqueous solution it was found that 90% of the peptide exists in *trans* conformation and thus only 10% of the available peptide could be used for the determination of rate of isomerization. In 1991 the assay was improved upon by Kofron *et al* [62]. Lower temperatures were introduced to reduce proteolytic cleavage of Pin1 and chymotrypsin as well as to reduce the rate of thermal conversion. Multiple wavelengths for absorbance measurements were also added to detect cleavage products at higher concentrations. Finally a novel solvent system of 50 mM HEPES, 0.1 M NaCl, and 5 mM NaN₃ was introduced which increases the available percentage of peptide in the *cis* conformation from 10:90 *cis:trans* to a reported 50:50 *cis:trans* ratio. The increase of peptide in the *cis* conformation increases the confidence these changes to the assay allow for a more accurate and efficient testing of Pin1 isomerase activity.

1.13 Thesis Overview

Throughout the literature, long peptide chains dominate as the preferred type of inhibitor for Pin1. These peptide chains exploit binding in the active site via the recognition sequence, as well as binding to sites on the periphery of the

active site. Designing competitive small molecule inhibitors presents a different challenge as the binding energy must be from a small area directly around the active site of the target protein. Previous research in this lab has shown that the substitution of pSer/pThr with β -phosphorylated glutamic acid increased binding to Pin1. This discovery opened doors for a new class of small molecule inhibitors for Pin1. Whereas previous inhibitors focused on modifying the proline position of the recognition sequence and residues removed from the active site. This new inhibitor focuses on increased binding through the modification of the pSer/pThr position.

Creating a small peptide inhibitor has advantages over the longer chain and highly hydrophobic peptides. The advantages include the diminished potential for non-selective interactions, the smaller inhibitor can potentially be altered with more ease than the larger chains, smaller molecules have the potential to require less time to synthesize, and synthesis of smaller molecules has the potential to be more cost effective. With all these potential advantages there is a higher chance that therapeutic or research-based use would increase.

The main goal of this research was to use rational design to synthesize novel inhibitors for Pin1. Using previous findings rational design was used to select proline analogues for substitution into Cbz-L-Glu(β -phos)-Pro-NH₂. The substitutions were then assessed for inhibitory potential against Pin1 activity. Centering the research on the novel β -phosphorylated inhibition strategy, we sought to increase the binding potential through utilizing the strategy of substitution at the proline position. It was thought that testing both successful

proline mimics in Pin1 inhibition studies, such as pipercolic acid, and novel proline substitutions, such as morpholine and methylpiperazine - both chosen in a rational design fashion, would render a strong, easily synthesized, inhibitor of Pin1.

Another goal was to increase the product yield of the Reformatsky addition in this application as low yields are unfavourable for a multi step synthesis.

This thesis will demonstrate the successful screening of four different C-terminal moieties coupled to β -phosphorylated glutamic acid, all of which are novel to Pin1 inhibition studies.

Chapter One References

1. Schonbrunner, E.R., et al., *Catalysis of protein folding by cyclophilins from different species*. J Biol Chem, 1991. **266**(6): p. 3630-5.
2. Gotherl, S.F. and M.A. Marahiel, *Peptidyl-prolyl cis-trans isomerases, a superfamily of ubiquitous folding catalysts*. Cell Mol Life Sci, 1999. **55**(3): p. 423-36.
3. Yaffe, M.B., et al., *Sequence-specific and phosphorylation-dependent proline isomerization: a potential mitotic regulatory mechanism*. Science, 1997. **278**(5345): p. 1957-60.
4. Wulf, G., et al., *Phosphorylation-specific prolyl isomerization: is there an underlying theme?* Nat Cell Biol, 2005. **7**(5): p. 435-41.
5. Kara Dolinski, Scott Muir, Maria Cardenas, Joseph Heitmanall *Cyclophilins and FK506 binding proteins are, individually and collectively, dispensable for viability in Saccharomyces cerevisiae*. Proc. Natl. Acad. Sci. USA 1997. **94** p. 13093-13098,
6. Barik, S., *Immunophilins: for the love of proteins*. Cell Mol Life Sci, 2006. **63**(24): p. 2889-900.
7. Bachinger, H.P., *The influence of peptidyl-prolyl cis-trans isomerase on the in vitro folding of type III collagen*. J Biol Chem, 1987. **262**(35): p. 17144-8.
8. Davis, J.M., B.A. Boswell, and H.P. Bachinger, *Thermal stability and folding of type IV procollagen and effect of peptidyl-prolyl cis-trans-isomerase on the folding of the triple helix*. J Biol Chem, 1989. **264**(15): p. 8956-62.
9. Steinmann, B., P. Bruckner, and A. Superti-Furga, *Cyclosporin A slows collagen triple-helix formation in vivo: indirect evidence for a physiologic role of peptidyl-prolyl cis-trans-isomerase*. J Biol Chem, 1991. **266**(2): p. 1299-303.
10. Kern, G., et al., *A kinetic analysis of the folding of human carbonic anhydrase II and its catalysis by cyclophilin*. J Biol Chem, 1995. **270**(2): p. 740-5.
11. Freskgard, P.O., et al., *Isomerase and chaperone activity of prolyl isomerase in the folding of carbonic anhydrase*. Science, 1992. **258**(5081): p. 466-8.
12. Tan, Y.J., et al., *The rate of isomerisation of peptidyl-proline bonds as a probe for interactions in the physiological denatured state of chymotrypsin inhibitor 2*. J Mol Biol, 1997. **269**(4): p. 611-22.
13. Kiefhaber, T., et al., *Folding of ribonuclease T1. 1. Existence of multiple unfolded states created by proline isomerization*. Biochemistry, 1990. **29**(12): p. 3053-61.
14. Rahfeld, J.U., et al., *Confirmation of the existence of a third family among peptidyl-prolyl cis/trans isomerases. Amino acid sequence and recombinant production of parvulin*. FEBS Lett, 1994. **352**(2): p. 180-4.

15. Rudd, K.E., et al., *A new family of peptidyl-prolyl isomerases*. Trends Biochem Sci, 1995. **20**(1): p. 12-4.
16. Lu, K.P., S.D. Hanes, and T. Hunter, *A human peptidyl-prolyl isomerase essential for regulation of mitosis*. Nature, 1996. **380**(6574): p. 544-7.
17. Winkler, K.E., et al., *Requirement of the prolyl isomerase Pin1 for the replication checkpoint*. Science, 2000. **287**(5458): p. 1644-7.
18. Liou, Y.C., et al., *Loss of Pin1 function in the mouse causes phenotypes resembling cyclin D1-null phenotypes*. Proc Natl Acad Sci U S A, 2002. **99**(3): p. 1335-40.
19. Esnault, S., et al., *The peptidyl-prolyl isomerase Pin1 regulates granulocyte-macrophage colony-stimulating factor mRNA stability in T lymphocytes*. J Immunol, 2006. **177**(10): p. 6999-7006.
20. Shen, Z.J., et al., *Pin1 regulates TGF-beta1 production by activated human and murine eosinophils and contributes to allergic lung fibrosis*. J Clin Invest, 2008. **118**(2): p. 479-90.
21. Shen, Z.J., et al., *The peptidyl-prolyl isomerase Pin1 facilitates cytokine-induced survival of eosinophils by suppressing Bax activation*. Nat Immunol, 2009. **10**(3): p. 257-65.
22. Liou, Y.C., et al., *Role of the prolyl isomerase Pin1 in protecting against age-dependent neurodegeneration*. Nature, 2003. **424**(6948): p. 556-61.
23. Lu, P.J., et al., *The prolyl isomerase Pin1 restores the function of Alzheimer-associated phosphorylated tau protein*. Nature, 1999. **399**(6738): p. 784-8.
24. Watashi, K., et al., *Human immunodeficiency virus type 1 replication and regulation of APOBEC3G by peptidyl prolyl isomerase Pin1*. J Virol, 2008. **82**(20): p. 9928-36.
25. Wulf, G.M., et al., *Pin1 is overexpressed in breast cancer and cooperates with Ras signaling in increasing the transcriptional activity of c-Jun towards cyclin D1*. EMBO J, 2001. **20**(13): p. 3459-72.
26. Ranganathan, R., et al., *Structural and functional analysis of the mitotic rotamase Pin1 suggests substrate recognition is phosphorylation dependent*. Cell, 1997. **89**(6): p. 875-86.
27. Otte, L., et al., *WW domain sequence activity relationships identified using ligand recognition propensities of 42 WW domains*. Protein Sci, 2003. **12**(3): p. 491-500.
28. Jager, M., et al., *Influence of hPin1 WW N-terminal domain boundaries on function, protein stability, and folding*. Protein Sci, 2007. **16**(7): p. 1495-501.
29. Yaffe, M.B. and L.C. Cantley, *Signal transduction. Grabbing phosphoproteins*. Nature, 1999. **402**(6757): p. 30-1.
30. Maleszka, R., et al., *The dodo gene family encodes a novel protein involved in signal transduction and protein folding*. Gene, 1997. **203**(2): p. 89-93.
31. Jobichen, C., Liou, Y.C., Sivaraman, J., *Crystal structure of a mutant PIN1 PEPTIDYL-PROLYL CIS-TRANS ISOMERASE*. released 25-08-2009, not yet published.

32. Bayer, E., et al., *Structural analysis of the mitotic regulator hPin1 in solution: insights into domain architecture and substrate binding*. J Biol Chem, 2003. **278**(28): p. 26183-93.
33. Felicia A. Etzkorn, J.P.N., Yang Zhang, Xiaodong J. Wang, *Pin1: Inhibitors and Mechanism*, in *Understanding Biology Using Peptides*, S.E. Blondelle, Editor. 2005. p. 759-762.
34. Labeikovsky, W., et al., *Structure and dynamics of pin1 during catalysis by NMR*. J Mol Biol, 2007. **367**(5): p. 1370-81.
35. Shen, M., et al., *The essential mitotic peptidyl-prolyl isomerase Pin1 binds and regulates mitosis-specific phosphoproteins*. Genes Dev, 1998. **12**(5): p. 706-20.
36. Wells, N.J., et al., *The C-terminal domain of the Cdc2 inhibitory kinase Myt1 interacts with Cdc2 complexes and is required for inhibition of G(2)/M progression*. J Cell Sci, 1999. **112 (Pt 19)**: p. 3361-71.
37. Jones, E.V., M.J. Dickman, and A.J. Whitmarsh, *Regulation of p73-mediated apoptosis by c-Jun N-terminal kinase*. Biochem J, 2007. **405**(3): p. 617-23.
38. Wulf, G.M., et al., *Role of Pin1 in the regulation of p53 stability and p21 transactivation, and cell cycle checkpoints in response to DNA damage*. J Biol Chem, 2002. **277**(50): p. 47976-9.
39. Balastik, M., et al., *Pin1 in Alzheimer's disease: multiple substrates, one regulatory mechanism?* Biochim Biophys Acta, 2007. **1772**(4): p. 422-9.
40. Etzkorn, F.A., *Pin1 flips Alzheimer's switch*. ACS Chem Biol, 2006. **1**(4): p. 214-6.
41. Messenger, M.M., et al., *Interactions between protein kinase CK2 and Pin1. Evidence for phosphorylation-dependent interactions*. J Biol Chem, 2002. **277**(25): p. 23054-64.
42. Crenshaw, D.G., et al., *The mitotic peptidyl-prolyl isomerase, Pin1, interacts with Cdc25 and Plx1*. EMBO J, 1998. **17**(5): p. 1315-27.
43. Bao, L., et al., *Prevalent overexpression of prolyl isomerase Pin1 in human cancers*. Am J Pathol, 2004. **164**(5): p. 1727-37.
44. Behrens, M.I., C. Lendon, and C.M. Roe, *A common biological mechanism in cancer and Alzheimer's disease?* Curr Alzheimer Res, 2009. **6**(3): p. 196-204.
45. Sheehy, A.M., et al., *Isolation of a human gene that inhibits HIV-1 infection and is suppressed by the viral Vif protein*. Nature, 2002. **418**(6898): p. 646-50.
46. Hennig, L., Christner, C., Kipping, M., Schelbert, B., Rücknagel, K.P., Grabley, S., Küllertz, G., and Fischer, G., *Selective Inactivation of Parvulin-Like Peptidyl-Prolyl cis/transIsomerases by Juglone*. Biochemistry, 1998, **37** (17), pp 5953–5960
47. Paulsen, M.T. and M. Ljungman, *The natural toxin juglone causes degradation of p53 and induces rapid H2AX phosphorylation and cell death in human fibroblasts*. Toxicol Appl Pharmacol, 2005. **209**(1): p. 1-9.
48. Smet, C., Duckert, J., Wieruszeski, Landrieu, I., Buee, L., Lippens, G., Deprez, B., *Control of protein-protein interactions: structure-based*

- discovery of low molecular weight inhibitors of the interactions between Pin1 WW domain and phosphopeptides. *J. Med. Chem.*, 2005. **48**.
49. Guo, C.e.a., *Structure-based design of novel human Pin1 inhibitors (I)*. *Bioorganic & Medicinal Chemistry Letters*, 2009(19): p. 5613-5616.
 50. Wildemann, D., et al., *Nanomolar inhibitors of the peptidyl prolyl cis/trans isomerase Pin1 from combinatorial peptide libraries*. *J Med Chem*, 2006. **49**(7): p. 2147-50.
 51. Zhang, Y., et al., *Structural basis for high-affinity peptide inhibition of human Pin1*. *ACS Chem Biol*, 2007. **2**(5): p. 320-8.
 52. Yixin Zhang, Susanne Fußsel, Ulf Reimer, Mike Schutkowski, and Gunter Fischer., *Substrate-Based Design of Reversible Pin1 Inhibitors*. *Biochemistry* **2002**, *41*, p. 11868-11877
 53. Tao Liu, Yu Liu, Hung-Ying Kao, and Dehua Pei., *Membrane Permeable Cyclic Peptidyl Inhibitors against Human Peptidylprolyl Isomerase Pin.1* *J. Med. Chem.* 2010, **53**, 2494–2501
 54. Duncan KE, Dempsey BR, Killip LE, Adams J, Bailey ML, Lajoie GA, Litchfield DW, Brandl CJ, Shaw GS, Shilton BH. *Discovery and characterization of a nonphosphorylated cyclic Peptide inhibitor of the peptidylprolyl isomerase, pin1*. *J Med Chem.* 2011 Jun 9;**54**(11):3854-65
 55. Wang, X.J., et al., *Conformationally locked isostere of phosphoSer-cis-Pro inhibits Pin1 23-fold better than phosphoSer-trans-Pro isostere*. *J Am Chem Soc*, 2004. **126**(47): p. 15533-42.
 56. Uchida, T., et al., *Pin1 and Par14 peptidyl prolyl isomerase inhibitors block cell proliferation*. *Chem Biol*, 2003. **10**(1): p. 15-24.
 57. Blaskovich, M.A., Lajoie, G.A. , *Synthesis of a chiral serine aldehyde equivalent and its conversion to chiral .alpha.-amino acid derivatives*. *J. Am. Chem. Soc.*, 1993. **115** (12): p. pp 5021–5030.
 58. Cram, D.J., Elhafez, F. A. A., *The rule of "Steric Control of Asymmetric Induction" in the Syntheses of Acyclic Systems*. *J. Am. Chem. Soc.*, 1952. **23**(74): p. 5828-5835.
 59. Anh and O. Eisenstein, *Nouv. J. Chim.*, 1977, **1**, 61
 60. Merrifield, R.B., *Solid Phase Peptide Synthesis. I. The Synthesis of a Tetrapeptide*. *J. Am. Chem. Soc.*, 1963. **85** (14).
 61. Janowski, B., Wollner, S., Schutkowski, M., Fischer, G., *a Protease-Free Assay for Peptidyl Proylcis/transisomerases Using standard Peptide Substrates*. *Analytical Biochemistry*, 1997. **252**(2): p. 299-307.
 62. Kofron, J.L., et al., *Determination of kinetic constants for peptidyl prolyl cis-trans isomerases by an improved spectrophotometric assay*. *Biochemistry*, 1991. **30**(25): p. 6127-34.

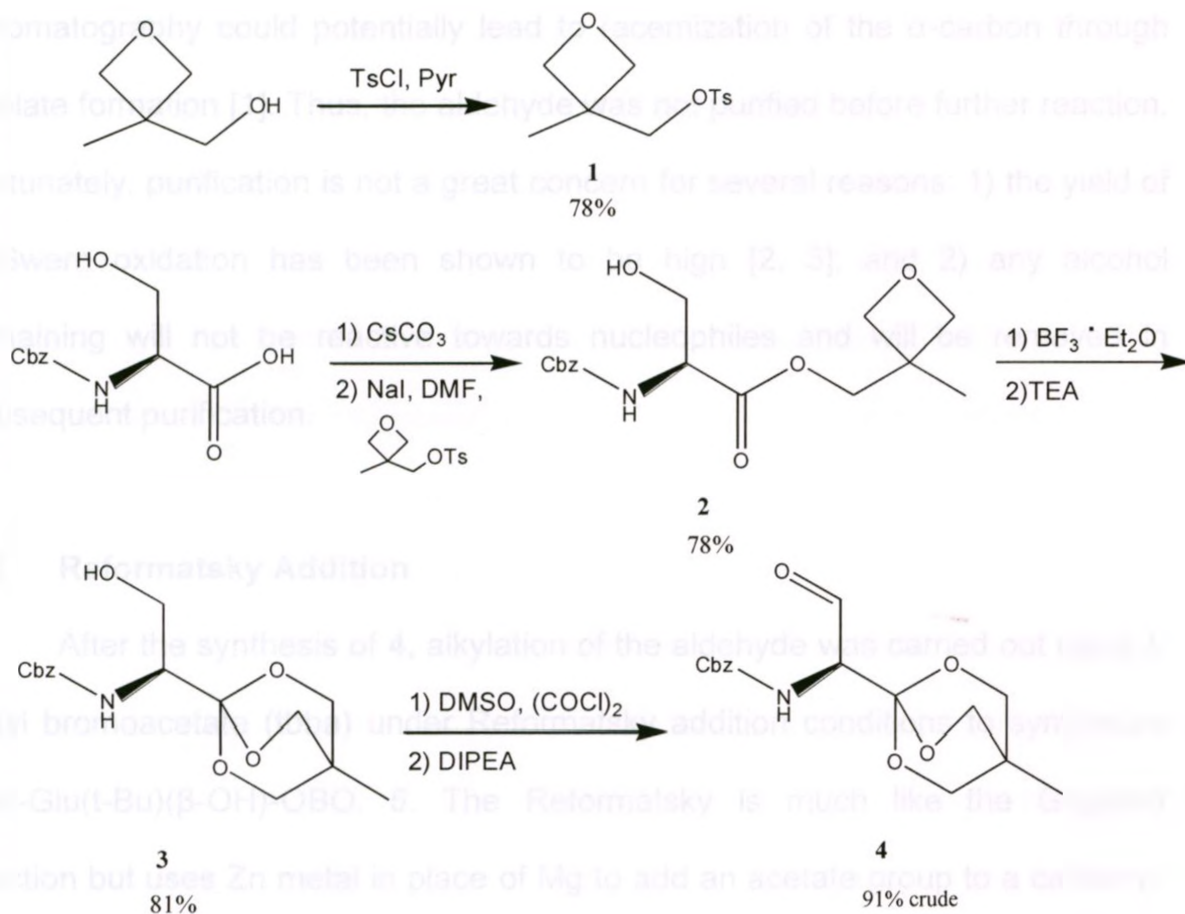
Chapter Two: Results & Discussion

2.1 Synthesis of N, C Protected Serine Aldehyde

Previous work in this lab determined that Cbz-Glu(β -phos)-Pro-NH₂ was active against Pin1 isomerase activity ($K_i = 20.0 \pm 0.9 \mu\text{M}$). It was hypothesized that the magnitude of inhibition could be increased through substituting the proline with structural analogs through stronger interaction with the active site of Pin1. To test this hypothesis four novel dipeptides, which are based on the β -hydroxyl substituted glutamic acid core molecule, were synthesized.

In 1993 Blaskovich and Lajoie [1] published a novel methodology for the synthesis of non-proteinaceous, β -substituted α -amino acids. The method utilized an OBO ester (4-methyl-2, 6, 7-trioxabicyclo[2.2.2]octane ester) as the carboxyl group protector. The OBO ester provides 1) protection from racemization at the α -carbon through reduction of α -hydrogen acidity, and 2) aids in the stereoselective addition to the β -carbon. The β aldehyde of serine is an excellent intermediate as it allows for the addition to the β -carbon using different strategies such as the Reformatsky reaction or Grignard reaction.

Scheme 2.1



The starting material, oxetane tosylate, **1**, was prepared on large scale, 20 g, with high yield (78%) through the addition of 3-methyl-3-(hydroxymethyl)oxetane to p-toluenesulfonyl chloride in the presence of pyridine. Cbz-serine oxetane ester, **2**, was then synthesized through the addition of **1** to Cbz-Ser through the formation of a cesium salt, catalyzed by the presence of the iodide ion (78%). To complete the protection of the carboxylic acid, the oxetane ester, **2**, was rearranged to the OBO ester using BF_3 as a Lewis acid catalyst

(81%). The β -hydroxyl was converted to a β -aldehyde under Swern oxidation conditions (crude yield of 91%). Purification of the aldehyde, **4**, through chromatography could potentially lead to racemization of the α -carbon through enolate formation [1]. Thus, the aldehyde was not purified before further reaction. Fortunately, purification is not a great concern for several reasons: 1) the yield of a Swern oxidation has been shown to be high [2, 3]; and 2) any alcohol remaining will not be reactive towards nucleophiles and will be removed in subsequent purification.

2.2 Reformatsky Addition

After the synthesis of **4**, alkylation of the aldehyde was carried out using *t*-butyl bromoacetate (tbba) under Reformatsky addition conditions to synthesize Cbz-Glu(*t*-Bu)(β -OH)-OBO, **5**. The Reformatsky is much like the Grignard reaction but uses Zn metal in place of Mg to add an acetate group to a carbonyl. Previous reports presented a yield of 27%; however, the reaction yielded enough material to continue with the synthesis to the final product. In that instance only one inhibitor was synthesized using the Reformatsky addition and the low yield was not investigated. For our purposes ca. 30% yield is a waste of starting materials and not synthetically favourable. Initial attempts using the prescribed method yielded 33%, which is still too low for a multi-step synthetic process. Potential problems could be one, or a combination, of: water contamination; low yield of the Swern oxidation; incomplete consumption of the reactants; improper ratios of reactants; and zinc purity.

Water contamination would cause a "quenching" of the reaction, and thus could result in low yields. As one of the simplest and most logical problems to address, fresh reagents were dried using molecular sieves in septum bottles and handled under argon to ensure that moisture in the air was not contaminating the reactants. A source of water could also have come from the aldehyde product. Cbz-Ser(ald)-OBO, **4**, was reconstituted in freshly distilled CH_2Cl_2 and dried over MgSO_4 before the solvent was removed *in vacuo* and then placed under high vacuum. The apparatus for the reaction was improved by using a two-neck round bottom flask (RBF) and introducing a stopcock to the second neck under argon flow, to allow addition of reactants without exposing the reaction to atmosphere. Performing the Reformatsky with carefully dried reagents and new apparatus yielded no significant change (34%). Water contamination did not seem to be the problem. However, the use of fresh dry reagents is always recommended. Thus, the carefully dried reagents and the improved apparatus were used for the remaining trials.

The purity of Zn was addressed next. Zn metal was cleaned in concentrated HCl to remove any oxide, washed with 50%, 70% and 99% EtOH/ H_2O solutions, rinsed twice with MeOH and dried at 110°C . The Reformatsky reaction with purified Zn metal yielded no change (31%). Purified Zn was used for the remainder of all subsequent reactions.

The Swern oxidation has been shown to be very effective and result in a high yield in different applications [2, 3]. However, having an ineffective oxidation process would lead to low yields in the Reformatsky addition. To determine if the

aldehyde was the cause of the low yield of the Reformatsky reaction the efficacy of the oxidation process had to be ascertained. Using TLC as an indicator to determine completion was not very effective as the aldehyde tended to streak on the plate. High resolution mass spectrometry also indicated that the product Cbz-*L*-Ser(ald)-OBO was synthesized; however, it does not rule out low yield as mass spectrometry is not quantitative. Fortunately, with ^1H NMR one can directly compare the spectra of Cbz-*L*-Ser-OBO, **3**, and Cbz-*L*-Ser(ald)-OBO, **4**. It is evident in the Cbz-*L*-Ser(ald)-OBO that the oxidation had been successful through the gain of a signal peak at 9.69 ppm, which is indicative of an aldehyde. Complementing the gain of an aldehyde peak would be the loss of the hydroxyl and the β -hydrogens signal as well. Both the loss of the hydroxyl peak at 2.51 ppm as well as the loss of the peak at 2.55 ppm which represented the pair of β -hydrogens can be clearly seen. Please refer to Figures 2.1 and 2.2 for ^1H NMR spectra of Cbz-*L*-Ser-OBO, **3**, and Cbz-*L*-Ser(ald)-OBO, **4**, respectively.

Figure 2.1-400 MHz ^1H NMR of Cbz-*L*-Ser-OBO (**3**)

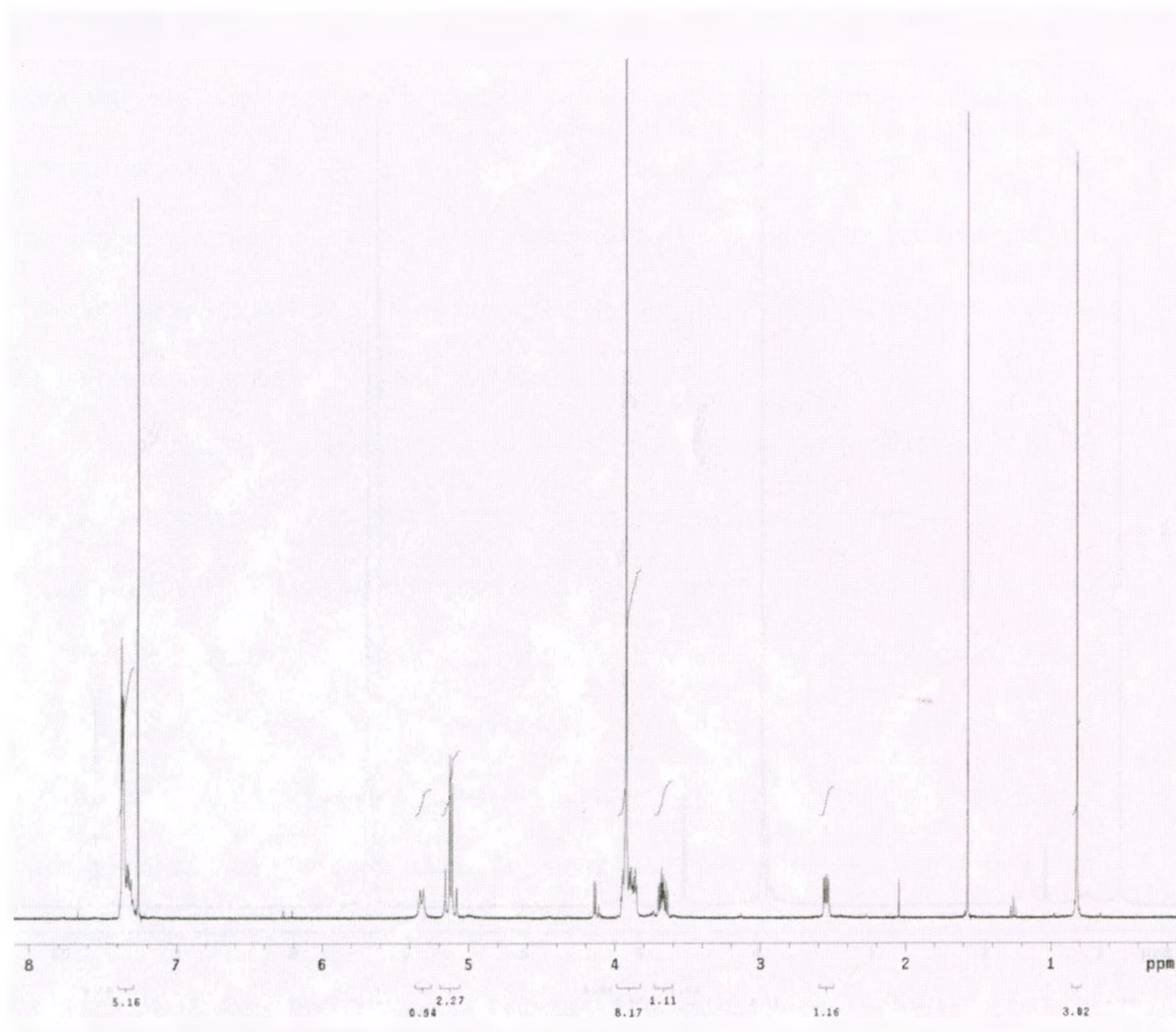


Figure 2.1 400 MHz ¹H NMR, CDCl₃, of Cbz-L-Ser-OBO, **3**.

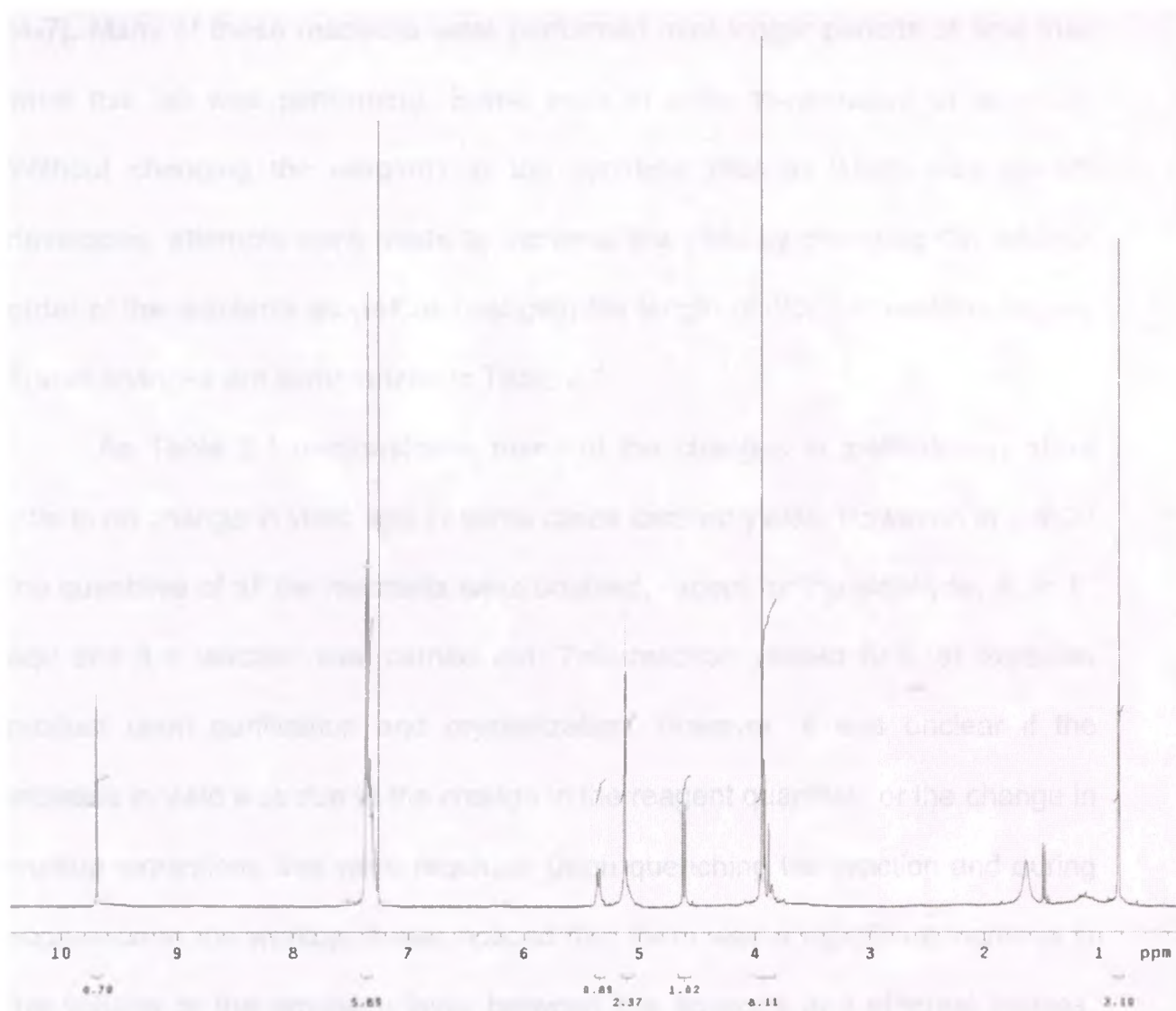


Figure 2.2 400 MHz ¹H NMR, CDCl₃, of Cbz-L-Ser(ald)-OBO, **4**.

If the reaction had been of low yield the ¹H NMR spectrum of Cbz-L-Ser(ald)-OBO would contain peaks belonging to both Cbz-L-Ser(ald)-OBO as well as Cbz-L-Ser-OBO. As the evidence supports that the oxidation was successful it was thought that the methodology of the Reformatsky addition was faulty. A survey of the literature revealed that different methods (including different reagents) were used to achieve Reformatsky additions with higher yields

[4-7]. Many of these reactions were performed over longer periods of time than what this lab was performing. Some were at room temperature or at reflux. Without changing the reagents in the synthetic process which was already developed, attempts were made to increase the yield by changing the addition order of the reactants as well as changing the length of different reaction stages. These changes are summarized in Table 2.1.

As Table 2.1 demonstrates many of the changes in methodology show little to no change in yield, and in some cases lowered yields. However, in trial 27 the quantities of all the reactants were doubled, except for the aldehyde, **4**, to 10 equ and the reaction was carried out. This reaction yielded 64% of expected product upon purification and crystallization. However, it was unclear if the increase in yield was due to the change in the reagent quantities or the change in workup extractions that were required. Upon quenching the reaction and during separation in the workup, it was noticed that there was a significant increase in the volume of the emulsion layer between the aqueous and ethereal phases. This layer of insoluble material was not unexpected, as it was present in all previous workups. However, the increased amount of material proved to be a challenge in easily separating the layers. As a result more extraction steps with CH_2Cl_2 were required to properly separate the two layers. With the increased volume of insoluble matter it was noticeable that during each subsequent extraction step the emulsion became whiter and less 'fluffy'. This change was not immediately apparent in the smaller quantities.

| Trials | Initial reactants (equ) | Conditions | Additional reactants (equ) | Reaction Duration (Reflux : cool down) | Yield (%) |
|--------|--|---|--------------------------------|--|-----------|
| 1-3 | Zn (5 equ), Iodine (cat) | reflux for 10 mins | tbba (5 equ), Aldehyde (1 equ) | 20:30 | 28-30 |
| 4-6 | Zn (5 equ), Iodine (cat) | reflux for 10 mins | tbba (5 equ), Aldehyde (1 equ) | 40:30 | 19-25 |
| 7-10 | Zn (5 equ), Iodine (cat) | reflux for 10 mins | tbba (5 equ), Aldehyde (1 equ) | 60:40 | 21-26 |
| 11 | Zn (5 equ), Iodine (cat), tbba (5 equ) | reflux for 10 mins | Aldehyde (1 equ) | 20:30 | 27 |
| 12-15 | Zn (5 equ), Iodine (cat), tbba (5 equ) | reflux for 20 mins | Aldehyde (1 equ) | 40:30 | 29-32 |
| 16,17 | Zn (5 equ), Iodine (cat), tbba (5 equ) | reflux for 20 mins | Aldehyde (1 equ) | 60:30 | 22-36 |
| 18,19 | Zn (5 equ), Iodine (cat), tbba (5 equ) | reflux for 20 mins | Aldehyde (1 equ) | 60:60 | 27-31 |
| 20 | Zn (5 equ), Iodine (cat), Aldehyde (1 equ) | reflux for 10 mins | tbba (5 equ) | 20:30 | 14 |
| 21-24 | Zn (5 equ), Iodine (cat), tbba (5 equ) | heated Zn and Iodine to reflux then added tbba and refluxed for 15 mins | Aldehyde (1 equ) | 20:30 | 31-32 |
| 25,26 | Zn (6 equ), Iodine (cat), tbba (6 equ) | heated Zn and Iodine to reflux then added tbba and refluxed for 15 mins | Aldehyde (1 equ) | 40:30 | 30-35 |

Table 2.1 Continued on next page

| | | | | | |
|------|--|--|----------------------------------|-------|-------|
| 27 * | Zn (10 equ), Iodine (cat), tbba (10 equ) | heated Zn and Iodine to reflux then added tbba and refluxed for 25 mins | Aldehyde (1 equ) | 40:60 | 64 |
| 28 * | Zn (5 equ), Iodine (cat) | reflux for 10 mins | Aldehyde (1 equ) tbba (5 equ) | 20:30 | 58 |
| 29 * | Zn (5 equ), Iodine (cat), tbba (5 equ) | heated Zn and Iodine to reflux then added tbba and refluxed for 25 mins | Aldehyde (1 equ) | 20:30 | 56-67 |

Table 2.1 Summary of methods attempted. The * denotes trials which were performed with additional washing steps.

To verify, the reaction was performed using the original five equivalents of reactants but the workup was altered to include extra extraction steps using CH_2Cl_2 (trial 28). Again, it was noticed that upon each wash the emulsion became whiter and less expanded. Part-way through the separation, the precipitate was collected from the separatory funnel, rinsed with CH_2Cl_2 and the fraction was spotted on TLC plate and verified by MS. It was found that product, Cbz-Glu(t-butyl)(β -OH)-OBO, **5**, was indeed still present in the insoluble/emulsion layer. Changing the workup to include more extractions with CH_2Cl_2 yielded a maximum 68% product upon purification and crystallization.

It was found that the method used for trials 21-24 was the simplest to perform and the easiest to control. Separating the additions of the reactants, t-butyl bromoacetate and the aldehyde, lead to less unreacted Zn metal remaining in the reaction vessel after completion of the reaction. This change also allowed

for quicker additions of the reactants to the reaction vessel minimizing exposure to atmosphere.

The stereochemical selectivity for this particular example can be directly explained using Cram's model, the Felkin-Anh model as well as 1,2 chelation control. Figure 2.3 demonstrates the Cram conformation (Figure 2.3 - A), the most probable conformation using the Felkin-Anh model (Figure 2.3 - B), and possible conformations using a 1,2 chelation control mechanism (Figure 2.3 - C and D). The use of the highly coordinating Zn metal, the configuration of the preexisting stereocenter of the α -carbon, the steric bulk of the OBO ester, and the existence of a free electron pair on the amide nitrogen all provide excellent conditions for 1,2 chelation control. Both possible configurations of 1,2 chelation control render the same stereocenter in the product (Figure 2.3 - E). In addition, the Felkin-Anh conformation model is also one of the configurations for 1,2 chelation control.

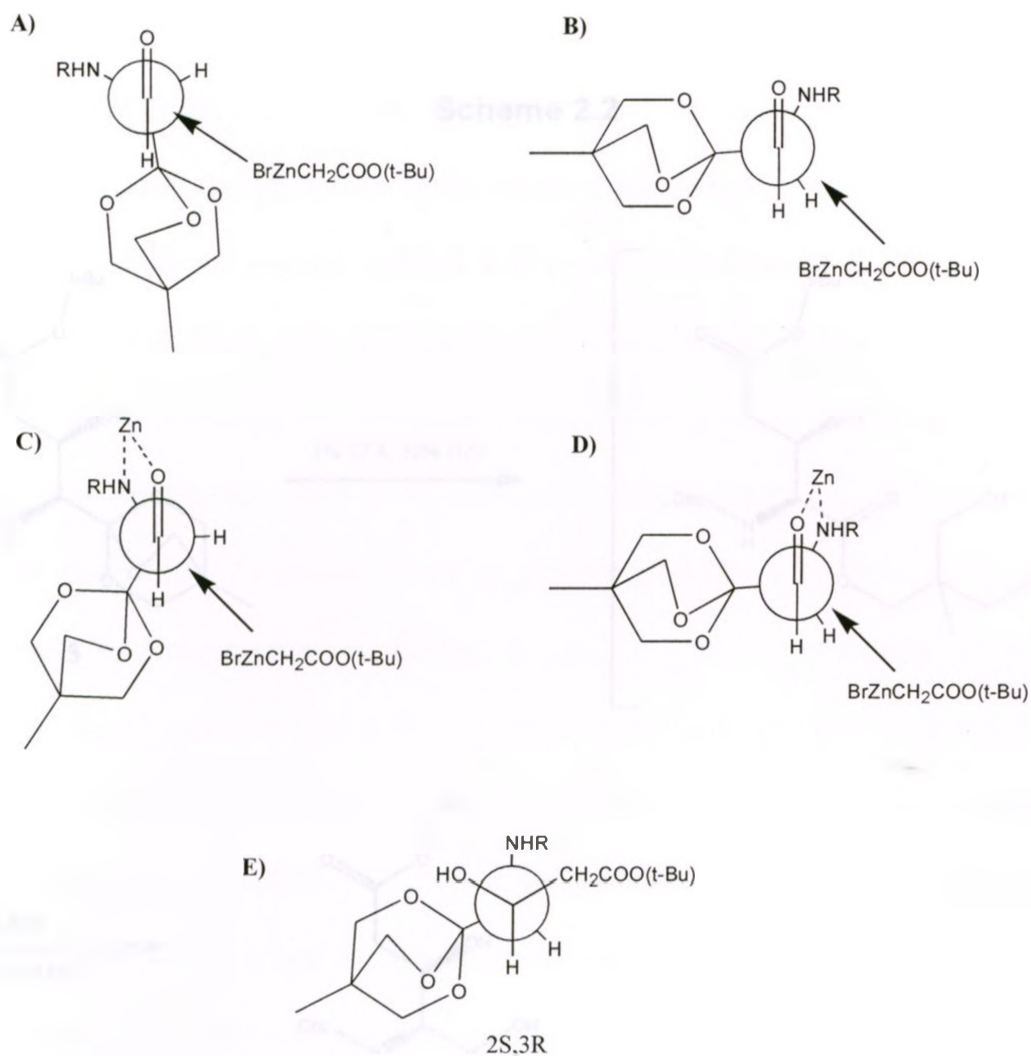
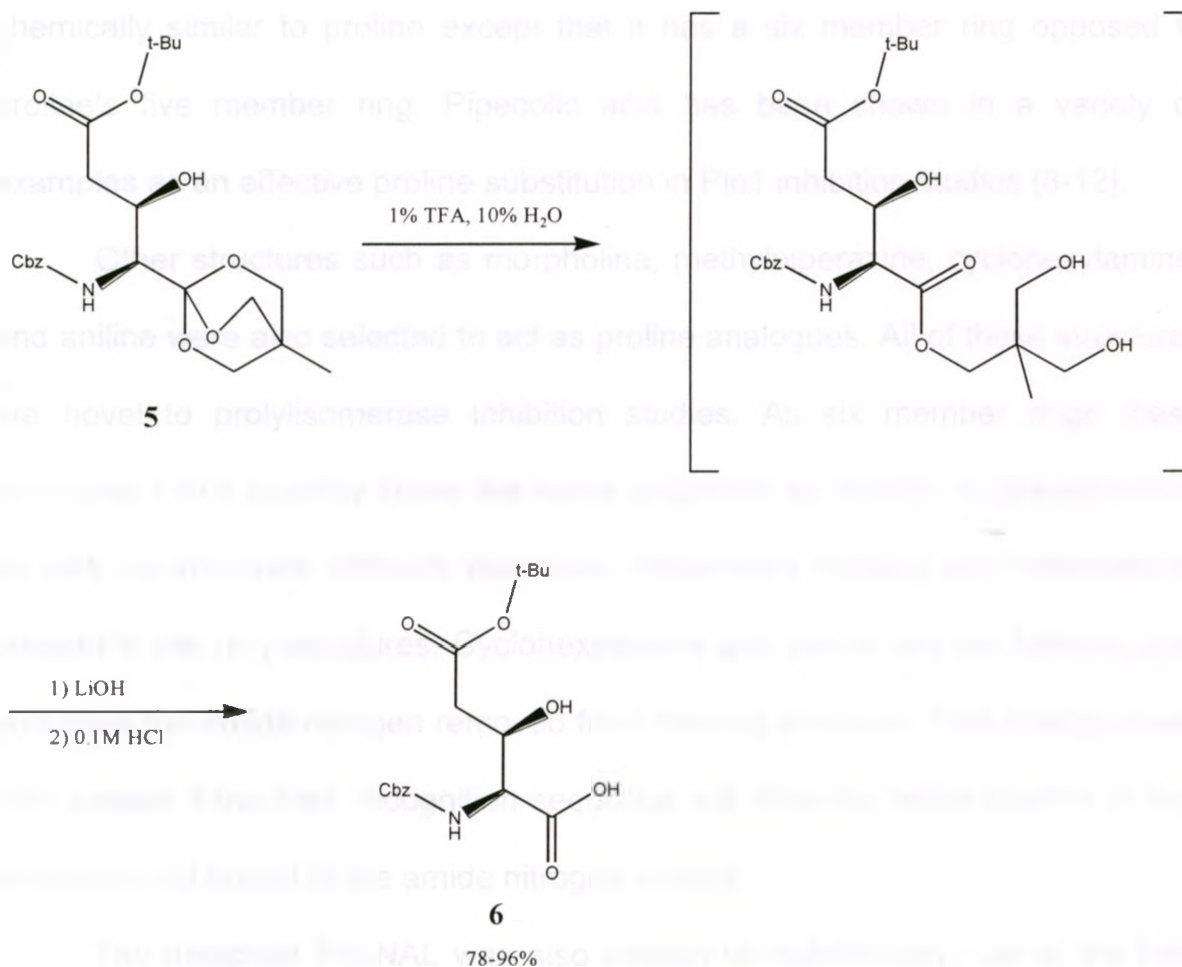


Figure 2.3 Newman projections showing addition to Cbz-Ser(ald)-OBO using A) Cram's rule, B) most probable addition using the Felkin-Anh model, C/D) possible conformations of addition using a 1,2 chelation control mechanism E) Newman projection of the major product formed, **5**. Where R is the Cbz protecting group.

2.3 Synthesis of Cbz-Glu(t-butyl)(β -OH)-OH

Selective removal of the OBO ester from **5** was carried out by hydrolyzing the OBO ester to the 2-methyl-2-hydroxymethyl-1,3-propanediol (MPHD) ester (not separated) and then selectively removing the MHPD ester over the t-butyl ester using hydroxide mediated cleavage. Scheme 2.2 demonstrates this process.

Scheme 2.2



Purification of the free acid was found to be extremely difficult using previously reported methods (unpublished). It was found that purification using acetone as the eluent for chromatography was extremely difficult and recovery of product was extremely low. Using EtOAc as the eluent in a silica gel column was sufficient to separate the product from unwanted materials before crystallization (78-96%).

2.4 Selection of Pin1 Inhibitor Analogues

Several proline analogues were chosen to be tested for inhibition activity. The most obvious candidate for substitution was pipercolic acid. Pipercolic acid is chemically similar to proline except that it has a six member ring opposed to proline's five member ring. Pipercolic acid has been shown in a variety of examples as an effective proline substitution in Pin1 inhibition studies [8-12].

Other structures such as morpholine, methylpiperazine, cyclohexylamine, and aniline were also selected to act as proline analogues. All of these structures are novel to prolyl isomerase inhibition studies. As six member rings these structures could possibly share the same properties as proline or pipercolic acid, as well as introduce different electronic interactions through any heteroatoms present in the ring structures. Cyclohexylamine and aniline are not heterocycles and have the amide nitrogen removed from the ring structure. This change could help assess if the Pin1 recognition sequence will allow for better binding of ring structures not bound to the amide nitrogen directly.

The dipeptide Pip-NAL was also chosen for substitution, due to the high degree of success Zhang *et al* [8] had in developing peptide chain inhibitors crystals. The Pip-NAL core resolved in crystallographic data showed that the naphthyl side chain interacted with an accessory hydrophobic binding pocket adjacent to the proline binding pocket in the Pin1 active site. The choice to use this core was to demonstrate the effectiveness of the naphthylalanine binding and showcase the novel β -substituted inhibitor design. Figure 2.4 demonstrates the different C-terminal structures

2.5 Synthesis of Pin1 Inhibitors

2.5.1 Solid Phase Preparation

Both pipercolic acid and NAL have terminal carboxylic acid functionality which allows for the convenient use of solid phase peptide synthesis.

2.5.1.1 Synthesis of Cbz-Glu(β -phos)-Pip-NH₂

N-protected pipercolic acid was coupled to the PAL solid support resin. Fmoc was removed from the pipercolic acid N-terminal and Cbz-Glu(t-butyl)(β -OH)-OH was coupled to the pipercolic acid. Both coupling steps utilized classical Fmoc chemistry reagents to couple the free N-terminal to the free C-terminal. The free hydroxyl was subsequently phosphorylated and oxidized using phosphoramidite class reagents. The dipeptide was cleaved from the resin and purified using HPLC yielding 5.8 mg of Cbz-Glu(β -phos)-Pip-NH₂, **17**.

2.5.1.2 Attempted Synthesis of Cbz-Glu(β -phos)-Pip-NAL-NH₂

Unfortunately the tripeptide, Cbz-Glu(β -phos)-Pip-NAL-NH₂, was not successfully synthesized. Using the same methods as synthesis of Cbz-Glu(β -phos)-Pip-NH₂, N-protected NAL was coupled to the PAL solid support resin. Fmoc was then removed from the NAL N-terminal and N-protected pipercolic acid was coupled to the NAL N-terminal. Fmoc was removed from pipercolic acid and Cbz-Glu(t-butyl)(β -OH)-OH was coupled to the growing chain. The free hydroxyl

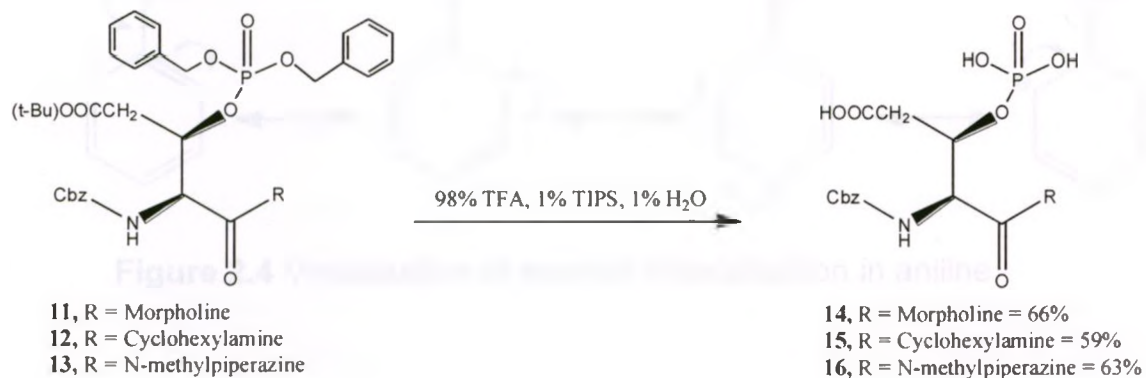
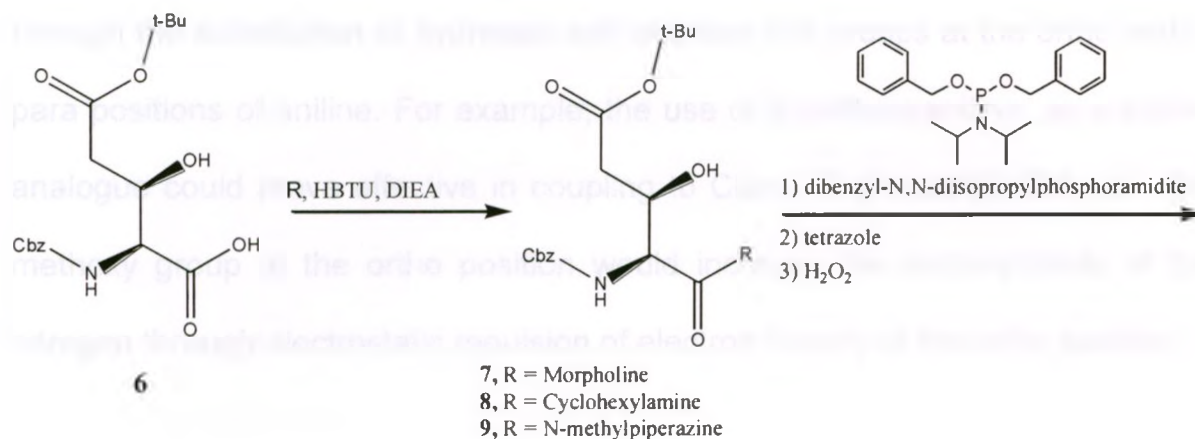
was subsequently phosphorylated and oxidized using phosphoramidite class reagents and H₂O₂ (*meta*-chloroperoxybenzoic acid (mCPBA) was initially used as an oxidizer. However, upon resin cleavage the process did not yield any product. The product was then cleaved from the resin, but the first attempt at synthesis failed to yield any detectable product. At each coupling step a verification of addition is completed by taking a small sample of the resin from the reaction vessel and performing a “mini-cleavage” of that resin. The products of the mini-cleavage are checked with mass spectrometry to detect the change in the peptide mass. The evidence suggested a loss of product occurred in the final steps of phosphorylation and oxidation. It was assumed that human error was the cause of the loss, most likely through an error in addition of the oxidizing agent mCPBA. The addition of too much oxidizer could cause premature cleavage off of the resin leading to a loss of product in the washing of the resin. Proceeding with the second attempt mCPBA was substituted with H₂O₂, which had proved successful for the synthesis of both Cbz-*L*-Glu(β -phos)-Pip-NH₂, **17**, and Cbz-*L*-Glu(β -phos)-Pro-NH₂. After several unsuccessful attempts, it was surmised that during the oxidation of the phosphite ether or during the cleavage from the resin, a side reaction was causing a decomposition of the product as there was no detectable product or intermediate in any wash waste or final cleavage.

2.5.2 Liquid Phase Preparation

Morpholine, methylpiperazine, cyclohexylamine, and aniline do not allow for the use of SPPS because there is no carboxylic acid functionality, or more

specifically, any other linkable and cleavable functionalities available for a solid phase synthesis resin. Thus, SPPS is not an option and liquid phase coupling must be used. Peptide coupling was completed by using 1 equ of Cbz-L-Glu(t-butyl)(β -OH)-OH, 1 equ HBTU, 1 equ DIPEA and 1.2 equ of a selected proline analogue. After coupling, the coupling reagents were removed using a very short silica column. The eluent was checked for coupled product, much like the mini-cleavage process in SPPS, and phosphorylation was completed using phosphoramidite class reagents. The protecting groups were then removed using TFA and products were purified using reverse phase HPLC. This process was done in a fashion similar to solid phase synthesis; intermediate products were checked by MS but were not collected until the end product (please see Scheme 2.3).

Scheme 2.3



The aromatic ring aniline failed to couple with success, even after 72 hours of continuous reaction. Checking the reaction status by MS indicated that the starting products were still present in the solution. The reason for the incomplete reaction can be explained by the aromaticity of the aniline ring diminishing the nucleophilicity of the amine. The delocalization of the charge

allows for several resonance structures which have a full positive charge on the nitrogen, preventing addition to a carboxylic acid (see Figure 2.4).

The distribution of charge around the aromatic ring can be reduced through the substitution of hydrogen with electron rich groups at the ortho and/or para positions of aniline. For example, the use of 2-methoxyaniline, as a proline analogue could prove effective in coupling to Cbz-L-Glu(t-butyl)(β -OH)-OH. The methoxy group at the ortho position would increase the nucleophilicity of the nitrogen through electrostatic repulsion of electron density at the ortho position.

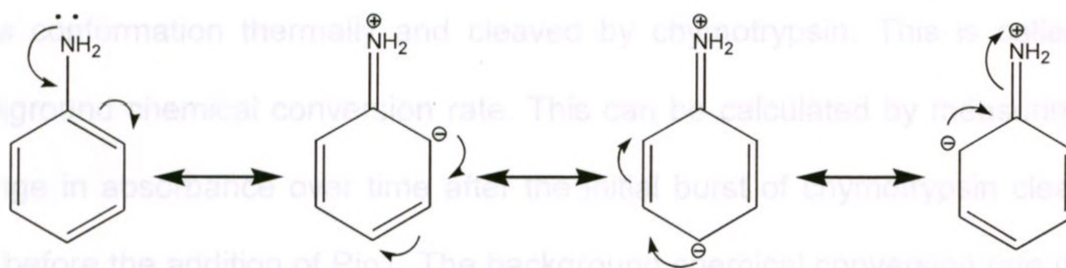


Figure 2.4 Visualization of electron delocalization in aniline.

Any alternate pursuits to couple aniline to Cbz-L-Glu(t-butyl)(β -OH)-OH were not made. Also, as the idea to utilize substituted aniline, regrettably, was generated at the time of writing, no attempts were made to couple Cbz-L-Glu(t-butyl)(β -OH)-OH to any aniline analogue.

2.6 Pin1 Inhibitor Activity

To test the inhibition potential of the synthesized molecules the chymotrypsin coupled photometric assay developed by Fischer *et al.* [13] and improved upon by Kofron *et al.* [14] was used.

The photospectrometer was equilibrated at 0°C. Pin1 substrate, suc-AEPF-pNA, was then added to the cuvette. After obtaining a baseline reading, chymotrypsin was then quickly added to the cuvette. As the substrate is a mixture of both the *cis* and *trans* conformations in solution, any substrate in the *trans* conformation was cleaved leaving only peptide in the *cis* form. During the assay there was a small percentage of substrate which was converted to the *trans* conformation thermally and cleaved by chymotrypsin. This is called the background chemical conversion rate. This can be calculated by measuring the change in absorbance over time after the initial burst of chymotrypsin cleavage and before the addition of Pin1. The background chemical conversion rate needs to be subtracted from the rate of Pin1 isomerization observed.

Pin1 was quickly added to the cuvette and the reaction was allowed to go to completion. The slope of the initial part of the curve was used to calculate the rate of Pin1 isomerization. (Please see Figure 2.5 for a visual representation of the tangents used to determine the rate of isomerization and the background chemical conversion rate.) Tangent slopes were determined by visual detection of the most linear portion of the curve and linear regression was used to ensure quality of the fit.

To determine the rate of isomerization the concentration of peptide in the *cis* conformation at the time of addition of Pin1 must be known. Because the concentration of free pNA in solution is dependent on the concentration of peptide which is cleaved, the concentrations of total peptide as well as the concentration of peptide in the *cis* conformation can be determined using Beer's law. The concentration of peptide in the *cis* conformation can be calculated by using the difference between the absorbance of just prior to the addition of Pin1 and the absorbance upon completion of the assay. To ensure that pNA cleavage is not the rate limiting step of the assay chymotrypsin is added in excess.

Once the rate of background chemical conversion and the initial rate of isomerization were calculated the data was plotted on a Michaelis-Menten plot. Constants are calculated through inversion of the plot to create a Lineweaver-Burk plot.

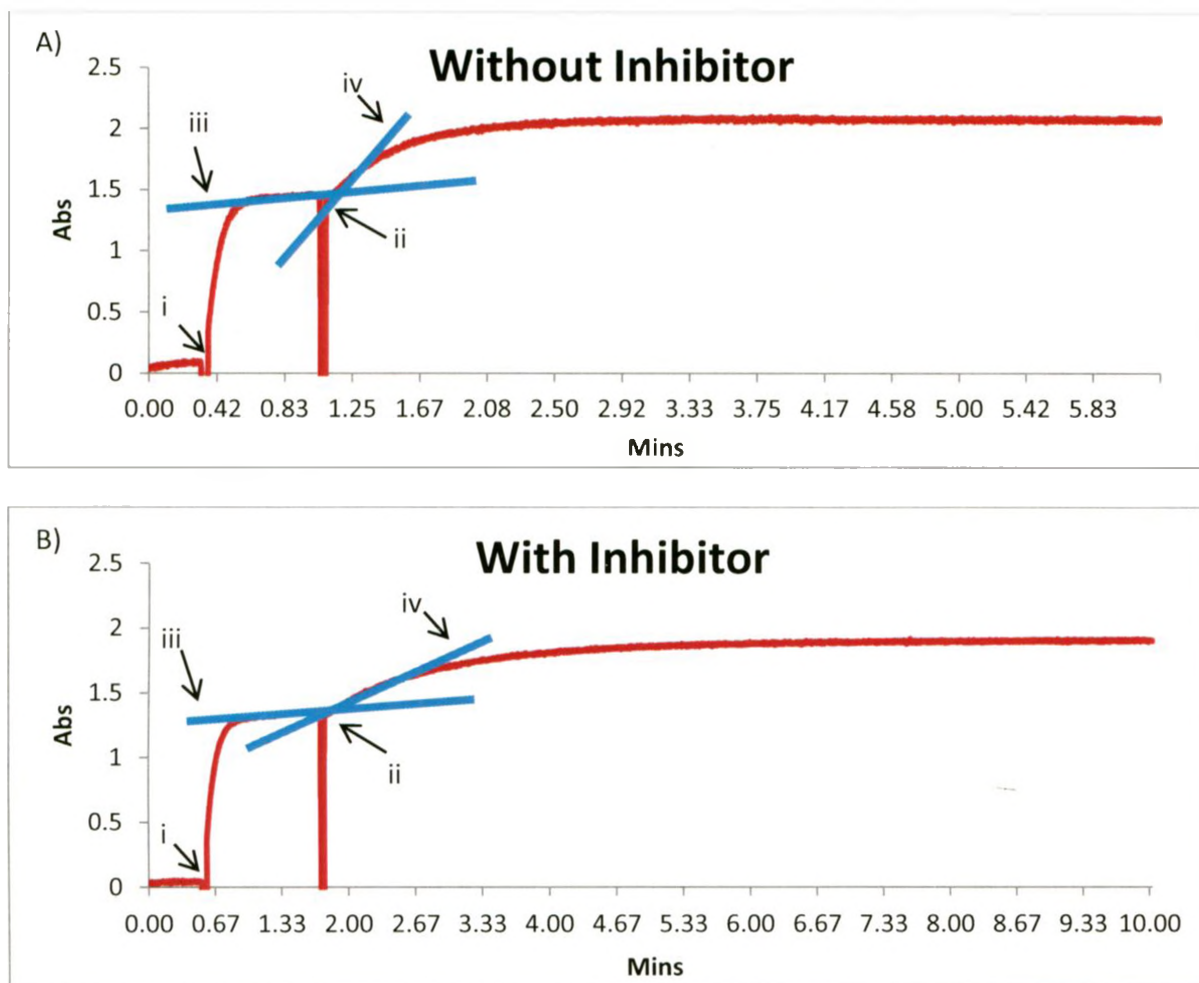


Figure 2.5 Sample raw data of chymotrypsin coupled Pin1 enzymatic assays. A) Representation of assay without inhibitor present. B) Assay in presence of Cbz-L-Glu(β -phos)-methylpiperazine. i represents time point where chymotrypsin is added, ii represents time point where Pin1 is added, iii represents the tangent line of the background chemical conversion rate, and iv represents the tangent line of the initial rate of Pin1 isomerization.

Substrate was added in increasing quantity to the cuvette to increase the concentration of available substrate in *cis* conformation. The amount of peptide in the *cis* conformation can never be duplicated exactly throughout runs as the concentration of *cis* peptide depends on many factors, such as, 1) the thermal conversion rate, 2) time between the addition of substrate and Pin1, and 3) the

amount of peptide in the *cis* conformation of the stock solution. For example, Figure 2.5 A and B are both examples of actual fluorescent data collected with the initial addition of the same concentration of total substrate. A) Represents data collected with the concentration of *cis* peptide determined to be 452 μM in the absence of an inhibitor and B) represents data collected with *cis* peptide at 395 μM in the presence of Cbz-L-Glu(β -phos)-methylpiperazine. The slope of the tangent lines ii and iv indicate the rate of background chemical conversion rate (iii) and the rate of initial isomerization of Pin1 (iv).

The results of the chymotrypsin coupled inhibition assays are presented in Table 2.2, along with a Michaelis-Menten plot of the different active inhibitors (Figure 2.6).

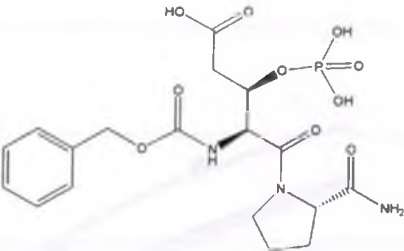
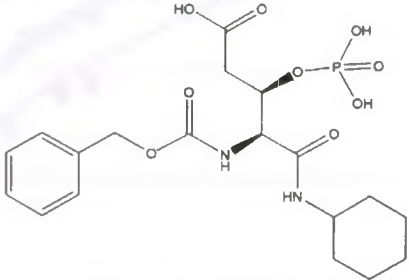
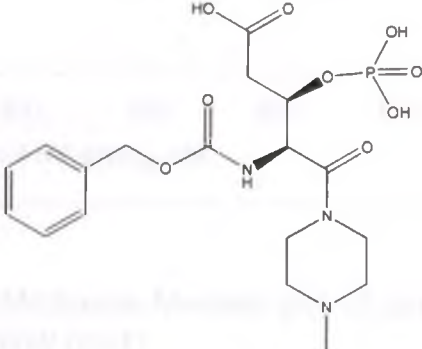
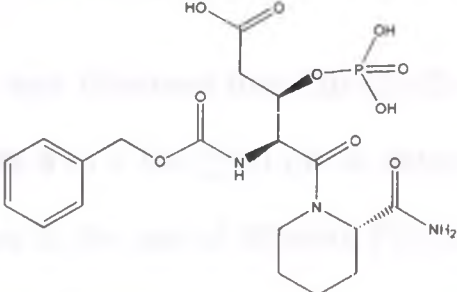
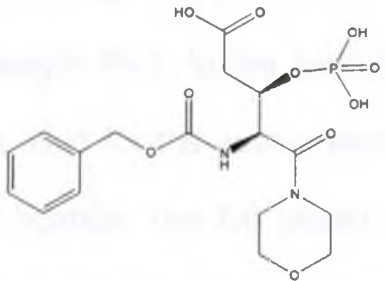
| Name | Structure | Inhibition (k_i) |
|--|--|------------------------|
| Cbz-L-Glu(β -phos)-Pro-NH ₂ |  <p>The structure shows a central chiral carbon atom bonded to a Cbz group (benzylloxycarbonyl), a phosphate group (beta-phosphate), and a proline ring. The proline ring has an amino group (-NH₂) attached to the nitrogen atom.</p> | 54.1 \pm 1.8 μ M |
| Cbz-L-Glu(β -phos)-cyclohexylamine 15 |  <p>The structure is similar to the first entry, but the proline ring is replaced by a cyclohexylamine ring.</p> | No inhibition |
| Cbz-L-Glu(β -phos)-methylpiperazine 16 |  <p>The structure is similar to the first entry, but the proline ring is replaced by a methylpiperazine ring.</p> | 22.7 \pm 1.4 μ M |
| Cbz-L-Glu(β -phos)-Pip-NH ₂ 17 |  <p>The structure is similar to the first entry, but the proline ring is replaced by a piperidine ring with an amino group (-NH₂) attached to the nitrogen atom.</p> | 45.4 \pm 1.1 μ M |
| Cbz-L-Glu(β -phos)-morpholine 14 |  <p>The structure is similar to the first entry, but the proline ring is replaced by a morpholine ring.</p> | No inhibition |

Table 2.2 Summary of Pin1 inhibition assays.

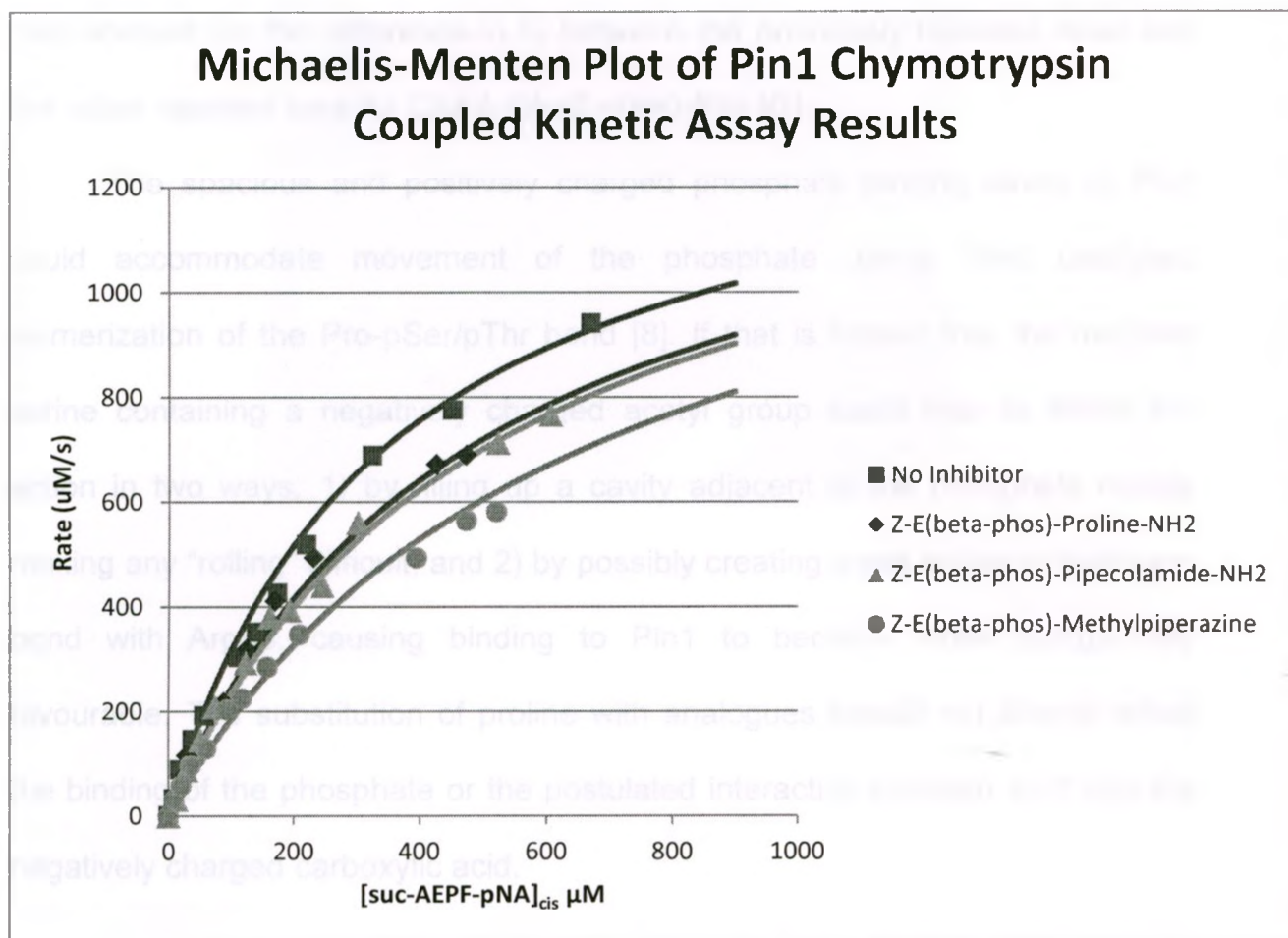


Figure 2.6 Pin1 inhibition Michaelis-Menten plot of synthesized inhibitors which demonstrated inhibition activity ($n=1$).

In previous work it was observed that Cbz-Glu(β -phos)-Pro-NH₂ exhibited a $K_i = 20.0 \pm 0.9 \mu\text{M}$, here a $K_i = 54.1 \pm 1.8 \mu\text{M}$ is determined. The difference in the value is most likely due to the use of different Pin1 stocks and isoforms. The chymotrypsin coupled kinetic assay was performed using the same procedure aside from the use of full length Pin1. In the previous study only the catalytic PPLase domain of Pin1 was used for the assay. Because the WW domain also binds to proline containing ligands, the full length enzyme would bind more inhibitor as well as substrate than just the single domain. These differences can

help account for the difference in K_i between the previously reported value and the value reported here for Cbz-L-Glu(β -phos)-Pro-NH₂.

The spacious and positively charged phosphate binding cavity in Pin1 could accommodate movement of the phosphate during Pin1 catalyzed isomerization of the Pro-pSer/pThr bond [8]. If that is indeed true the modified serine containing a negatively charged acetyl group could help to inhibit the action in two ways: 1) by filling up a cavity adjacent to the phosphate moiety making any "rolling" difficult; and 2) by possibly creating a salt bridge or hydrogen bond with Arg68, causing binding to Pin1 to become more energetically favourable. The substitution of proline with analogues should not directly affect the binding of the phosphate or the postulated interaction between Pin1 and the negatively charged carboxylic acid.

Analysis of the proline binding pocket of Pin1 structure published by Zhang *et al.* [8] (Figure 2.7), shows that there exists more room in the binding pocket opposite of the hydrophobic residues, towards His59 and His157. The "greasy" binding pocket formed by Leu122, Met130, and Phe134 allows for stronger hydrophobic interaction between the inhibitor and the enzyme.

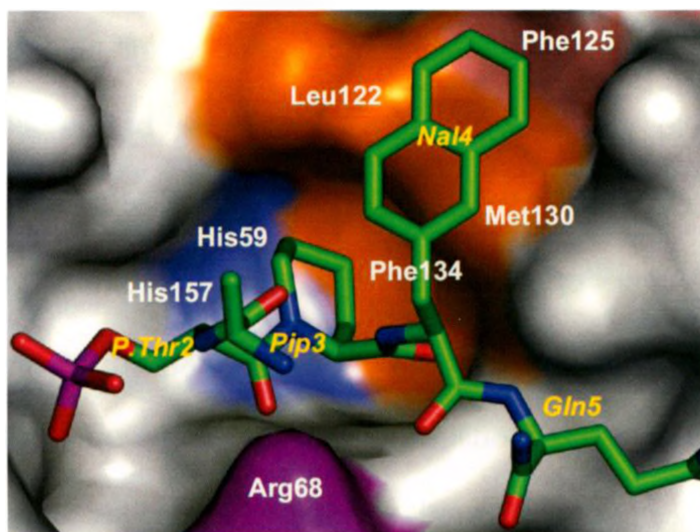


Figure 2.7 NMR structure of the binding pocket of Pin1. Bound to Pin1 is the peptide Ac-Phe-D-Thr(PO_3)-Pip-NAL-Gln- NH_2 (Thr(PO_3)-Pip-NAL-Gln shown) adapted from Zheng *et al.* [8].

Substituting proline for pipercolic acid increases the available surface area of the inhibitor and does not change the chemical properties substantially. The larger group could bind with higher affinity through more interaction with the enzyme. This substitution yields only a moderate increase in inhibition over -Glu(β -phos)-Pro- NH_2 .

Increased inhibition qualities of Cbz-L-Glu(β -phos)-methylpiperazine can be explained by: the increase in the available surface area for binding; the heterocyclic ring potentially allowing for hydrogen bonding between His157 and/or His59 and; the methyl group on the amine nitrogen could potentially protrude into the gap, towards Phe134, increasing interaction between the inhibitor and Pin1.

Both Cbz-Glu(β -phos)-morpholine and Cbz-Glu(β -phos)-cyclohexylamine do not show any inhibitory characteristics. Cbz-Glu(β -phos)-cyclohexylamine may not exhibit inhibition qualities due to the extra bond length between the ring

structure and the amide link as the nitrogen is not part of the cyclic structure as it is in proline. This added length may cause too much of an unfavourable difference in the structure to be recognized by the selective Pin1 recognition sequence, causing little to no binding of the molecule to Pin1. What is interesting is that Cbz-Glu(β -phos)-morpholine also showed no inhibition for PPLase activity. It was thought that the inclusion of morpholine would 1) be favourable for solubility in vivo, as well as 2) increase binding through hydrogen bonding potential with the dual histidines in the Pin1 binding pocket. If Cbz-Glu(β -phos)-morpholine is compared with Cbz-Glu(β -phos)-methylpiperazine it can be noticed that there is a high degree of similarity between the two structures. It is possible that the cyclic ether is not hydrophobic enough to cause sufficient binding to the greasy binding pocket, but perhaps the methyl group on Cbz-Glu(β -phos)-methylpiperazine increases the hydrophobicity of the heterocycle enough to allowing for binding.

Cbz-Glu(β -phos)-Pro-NH₂, Cbz-Glu(β -phos)-Pip-NH₂ and Cbz-Glu(β -phos)-methylpiperazine all differ from previously published inhibitors in that no inhibitors have utilized the β -carbon of Ser/Thr in the recognition sequence to increase binding potential. Either β -phosphorylated glutamic acid or the dipeptide Glu(β -phos)-Pip could be used in conjunction with other peptide based designs such as those explored by Zhang *et al.* [8], Guo *et al.* [11], Liu *et al.* [12], and Janowski *et al.* [15]. Duncan *et al.* [16] very recently published a paper exploring the use of non-phosphorylated cyclic peptides as Pin1 inhibitors. It would be of

interest to test a substitution of Glu(β -phos)-Pip in the cyclic peptide CRYPEVEIC at the Y-P position to determine if the peptide exhibited stronger inhibition. Although substituting β -phosphorylated glutamic acid would defeat the purpose of having a non-phosphorylated peptide, it would be interesting to see if there is any change in inhibitory potential if Glu(β -phos)-Pip is substituted into the cyclic peptide.

Unfortunately, due to the lack of a linkable group on methylpiperazine, the core of Cbz-Glu(β -phos)-methylpiperazine is not compatible with other peptide designs or strategies for Pin1 inhibition. However, if 4-Methyl-piperazine-2-carboxylic acid were to be used then it would be possible to link into a peptide chain. 4-Methyl-piperazine-2-carboxylic acid would contain the same functional groups thought to increase inhibition but would give the additional functionality of allowing a second peptide bond.

As an example, to compare Cbz-Glu(β -phos)-Pip-NH₂ and Cbz-Glu(β -phos)-methylpiperazine to compounds such as PiJ and PiB [17] (Figure 2.8) it can be easily seen that PiJ and PiB are highly hydrophobic compounds whereas Cbz-Glu(β -phos)-Pip-NH₂ and Cbz-Glu(β -phos)-methylpiperazine are not. The interaction of PiB and PiJ with Pin1 have been demonstrated using NMR [17], however, interactions with other enzymes are highly likely due to non-specific binding to hydrophobic surfaces on many different proteins. Also unlike PiB and PiJ, Cbz-Glu(β -phos)-Pip-NH₂ and Cbz-Glu(β -phos)-methylpiperazine are designed to be specific to the Pin1 recognition sequence. Hopefully, Cbz-Glu(β -

phos)-Pip-NH₂ and Cbz-Glu(β-phos)-methylpiperazine would have reduced non-specific interactions as they do not contain large hydrophobic groups.

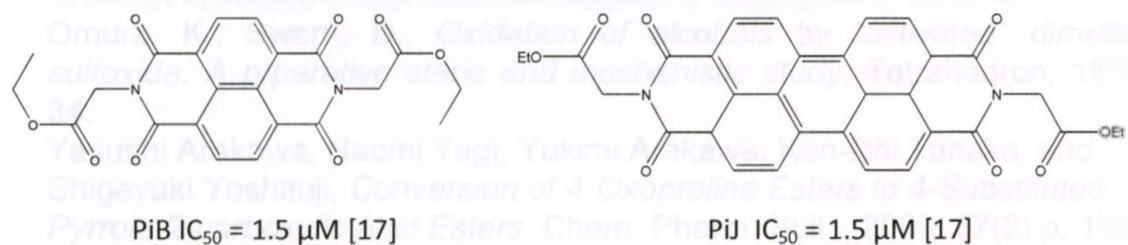


Figure 2.8 Structural representations of PiB and PiJ

One of the goals of this research was to test several proline analogues for stronger inhibition than Cbz-L-Glu(β-phos)-Pro-NH₂ ($K_i = 54.1 \pm 1.8 \mu\text{M}$), in the hopes of developing a sub μM range inhibitor. Unfortunately, we were unable to obtain a sub μM range inhibitor. However, Cbz-L-Glu(β-phos)-Pip-NH₂ ($K_i = 45.4 \pm 1.1 \mu\text{M}$) and Cbz-L-Glu(β-phos)-Methylpiperazine ($K_i = 22.7 \pm 1.4 \mu\text{M}$) both demonstrated a stronger inhibition of Pin1 than Cbz-L-Glu(β-phos)-Pro-NH₂.

Chapter Two References

1. Blaskovich, M.A., Lajoie, G.A. , *Synthesis of a chiral serine aldehyde equivalent and its conversion to chiral .alpha.-amino acid derivatives*. J. Am. Chem. Soc., 1993. **115** (12): p. pp 5021–5030.
2. Huang, S.L., Swern, D., *Preperation of iminosufuranes utilizing the dimethyl sulfoxide-oxalyl chloride reagent*. J. Org. Chem, 1978. **43**.
3. Omura, K., Swern, D., *Oxidation of alcohols by "activated" dimethyl sulfoxide. A prparative steric and mechanistic study*. Tetrahedron, 1978. **34**.
4. Yasushi Arakawa, Naomi Yagi, Yukimi Arakawa, Ken-ichi Tanaka, and Shigeyuki Yoshifuji, *Conversion of 4-Oxoproline Esters to 4-Substituted Pyrrole-2-carboxylic Acid Esters*. Chem. Pharm. Bull. , 2009. **57**(2) p. 167-176
5. M. Ángeles Fernández-Ibáñez, Beatriz Maciá, Adriaan J. Minnaard and Ben L. Feringa *Catalytic enantioselective Reformatsky reaction with ketones* Chem. Commun., 2008, p. 2571–2573
6. Srinivasarao Arulananda Babu, Makoto Yasuda, Ikuya Shibata, and Akio Baba, *In- or In(I)-Employed Tailoring of the Stereogenic Centers in the Reformatsky-Type Reactions of Simple Ketones, r-Alkoxy Ketones, and α -Keto Esters*. J. Org. Chem. 2005, **70**, 10408-10419
7. M. Ángeles Fernández-Ibáñez, Beatriz Maciá, Adriaan J. Minnaard and Ben L. Feringa, *Catalytic Enantioselective Reformatsky Reaction with ortho-Substituted Diarylketones*. Organic Letters 2008, **10** (18), p. 4041-4044
8. Zhang, Y., et al., *Structural basis for high-affinity peptide inhibition of human Pin1*. ACS Chem Biol, 2007. **2**(5): p. 320-8.
9. Smet, C., Duckert, J., Wieruszkeski, Landrieu, I., Buee, L., Lippens, G., Deprez, B., *Control of Protein-Protein Interactions: Structure-Based Discovery of Low Molecular Weight Inhibitors of the Interactions between Pin1 WW Domain and Phosphopeptides*. J. Med. Chem., 2005. **48** p. 4815-4823
10. Guo, C., et al., *Structure-based design of novel human Pin1 inhibitors (I)*. Bioorganic & Medicinal Chemistry Letters, 2009(19): p. 5613-5616.
11. Wildemann, D., et al., *Nanomolar inhibitors of the peptidyl prolyl cis/trans isomerase Pin1 from combinatorial peptide libraries*. J Med Chem, 2006. **49**(7): p. 2147-50.
12. Tao Liu, Yu Liu, Hung-Ying Kao, and Dehua Pei., *Membrane Permeable Cyclic Peptidyl Inhibitors against Human Peptidylprolyl Isomerase Pin.1* J. Med. Chem. 2010, **53**, 2494–2501
13. Kofron, J.L., et al., *Determination of kinetic constants for peptidyl prolyl cis-trans isomerases by an improved spectrophotometric assay*. Biochemistry, 1991. **30**(25): p. 6127-34.

14. Janowski, B., Wollner, S., Schutkowski, M., Fischer, G., *a Protease-Free Assay for Peptidyl Prolyl/trans Isomerases Using standard Peptide Substrates*. Analytical Biochemistry, 1997. **252**(2): p. 299-307.
15. Yixin Zhang, Susanne Fu"ssel, Ulf Reimer, Mike Schutkowski, and Gunter Fischer., *Substrate-Based Design of Reversible Pin1 Inhibitors*. *Biochemistry* **2002**, *41*, p. 11868-1187
16. Duncan KE, Dempsey BR, Killip LE, Adams J, Bailey ML, Lajoie GA, Litchfield DW, Brandl CJ, Shaw GS, Shilton BH. *Discovery and characterization of a nonphosphorylated cyclic Peptide inhibitor of the peptidylprolyl isomerase, pin1*. J Med Chem. 2011 Jun 9;54(11):3854-65
17. Uchida, T et al. *Pin1 and Par14 Peptidyl Prolyl Isomerase Inhibitors Block Cell Proliferation*, Chem. Biol. 2003, **10**, p. 15-24

Chapter Three: Experimental Section

3.1 Instrumentation

NMR spectra were collected using acetone- d_6 (referenced to 2.05 ppm for ^1H NMR, 29.9 ppm for ^{13}C NMR), CDCl_3 (referenced to TMS at 0.00 ppm for ^1H NMR, to CDCl_3 at 77.23 ppm for ^{13}C NMR), or D_2O (referenced to 3-(trimethylsilyl)propionic-2,2,3,3- d_4 acid at 0.00 ppm for both ^1H NMR and ^{13}C NMR) on a Varian Mercury 400 MHz spectrometer. For any NMR samples using CDCl_3 which contained an OBO ester, the CDCl_3 was pre-filtered through basic alumina to remove any traces of acid to retain product integrity during measurement.

Melting points were determined using a Mel-Temp melting temperature apparatus using open capillary tubes. Melting temperatures recorded are uncalibrated.

Mass spectral (MS) analyses were performed on a Micromass Quattro Micro ESI-MS instrument. Accurate mass/elemental analysis was carried out using a Varian QFT-12 FT-ICR.

TLC was carried out on EMD Chemicals Inc. aluminum backed silica gel 60 F₂₅₄, with visualization of spots by UV or a solution of 2% ninhydrin in MeOH and UV. Flash chromatography was performed with silica gel 60 (70-230 mesh) from EMD Chemicals Inc.

Semi-preparative HPLC analyses were performed using a Waters 600E HPLC system controller with a Waters 600 multisolvent delivery system and

detection was carried out using a Waters 2487 Dual λ absorbance detector. The column used was Agilent Zorbax 300SB-C18 (250x9.4mm, 5 μ m). Analytical HPLC analyses were performed using Agilent 1100 Series HPLC system with a Phenomenex Jupiter 5u C18 300A (250x2mm, 5 μ m) column coupled with the Micromass Quattro Micro ESI-MS to positively identify elution peaks.

3.2 Reagents

Triethylamine, oxalyl chloride, diisopropylethylamine, tetrahydrofuran, boron trifluoride etherate, pyridine, tert-butyl bromoacetate, ethyl acetate, trifluoroacetic acid, dibenzyl N,N-diethylphosphoramidite, dimethylsulfoxide, morpholine, 1-N-methylpiperazine, 3-methyl-3-oxetanemethanol (oxetane), cyclohexylamine, *meta*-chlorobenzoic acid, pipercolic acid were purchased from Sigma-Aldrich and used without any further purification.

Iodine, dimethylformamide, cesium carbonate, p-toluenesulfonyl chloride and sodium iodide were purchased from Caledon Labs and dichloromethane was purchased from J.T. Baker.

PAL amide resin was purchased from Advanced Chemtech; Cbz-serine and peptide coupling reagents HOBt and HBTU were purchased from Novabiochem.

Full Pin1 enzyme was collected and purified from recombinant *E. Coli* and graciously given by the Shilton lab.

3.3 Chemical Synthesis

3.3.1 Oxetane Tosylate, 1

3-Methyl-3-(toluenesulfonyloxymethyl)oxetane, Oxetane tosylate, **1**. 57.2 g (0.3 mol) of p-toluenesulfonyl chloride was dissolved in dry pyridine (250 mL) under argon. 3-Methyl-3-(hydroxymethyl)oxetane (20.4 g, 0.2 mol) was added slowly, and the solution was stirred for 1.5 h. The mixture was added slowly to a rapidly stirring mixture of deionized water (700 mL) and crushed ice (700 g,) in a 2 L Erlenmeyer flask and allowed to stir for an additional 0.5 h. The white precipitate was then vacuum filtered on Whatman filter paper # 1 and washed with cold H₂O. The product was dried under high vacuum to obtain the white powder of oxetane tosylate (36.8 g, 78%). Mp 48-50°C (lit 49.5-51°C [1]) ¹H NMR (CDCl₃, 400 MHz) δ 1.30 (s, 3H), 2.44 (s, 3H), 4.16 (s, 2H), 4.38 (m, 4H), 7.39 (d, 2H), 7.81 (d, 2H). High resolution MS calc'd for C₁₂H₁₆O₄S₁Na (M+Na⁺) 279.06615, found 279.06611 (M+Na⁺).

3.3.2 Cbz-L-Ser-Oxetane Ester, 2

2-Benzyloxycarbonylamino-3-hydroxypropionic acid 3-methyloxetane-3-ylmethyl ester, Cbz-L-Ser-Oxetane ester, **2**. **1** (11.36 g, 0.047 mol) and Cs₂CO₃ (9.19 g, 0.028 mol, 0.6 equ) were combined and dissolved in a 500 mL round bottomed flask (RBF) using 100 mL deionized H₂O. The water was then removed *in vacuo*, and the resulting oil was lyophilized for 12 h yielding white foam. The foam was then taken up in DMF (200 mL), oxetane tosylate, **1** (12.65 g, 0.049 mol) and NaI

(1.41 g, 9.8 mmol, 0.2 equ) were added and allowed to stir under Ar for 48 h. The DMF was then removed *in vacuo*, and the resulting solid was dissolved using alternating aliquots of EtOAc (600 mL total) and H₂O (200 mL total). The organic layer was separated and extracted with 10% NaHCO₃ (2x 100 mL) and saturated NaCl (1 × 100 mL), and then dried over MgSO₄. The solvent was removed under reduced pressure to yield a yellow oil which was recrystallized from Et₂O to yield colorless rod-like crystals in 78% yield (11.9 g). mp 62-64°C (lit [2] 58-60°C); [α]²⁰_D = -8.2 (c = 0.875, EtOAc) (lit [2] -8.3, c = 1.0, EtOAc); TLC (2:1, EtOAc:Hexane), R_f = 0.42; ¹H NMR (CDCl₃, 400 MHz) δ 1.26 (br s, 3H), 2.88 (t, 1H), 3.88-3.95 (br m, 1H), 4.07-4.17 (br m, 2H), 4.42-4.58 (br m, 6H), 5.14 (s, 2H), 5.74 (d, 1H), 7.28-7.40 (br m, 5H). High resolution MS calc'd for C₁₆H₂₁NO₆Na (M+Na⁺) 346.12611, found 346.12632 (M+Na⁺).

3.3.3 Cbz-L-Ser-OBO Ester, 3

[2-Hydroxy-1-(4-methyl-2,6,7-trioxa-bicyclo[2.2.2]oct-1-yl)-ethyl]-carbamic acid benzyl ester, Cbz-L-Ser-OBO ester, **3**. Cbz-L-Ser-Oxetane ester, **2** (12.14 g, 36.6 mmol) was dissolved in dry CH₂Cl₂ (450 mL) and cooled to 0 °C under Ar. BF₃·Et₂O (0.23 mL, 1.83 mmol) was diluted in CH₂Cl₂ (5.0 mL) and added to the reaction flask. The reaction was allowed to warm to room temperature and was checked by TLC. After 6 h, Et₃N (1.28 mL, 9.15 mmol) was added and the reaction was stirred for an additional 30 min before being concentrated *in vacuo* to a thick clear oil. The crude product was re-dissolved in EtOAc (400 mL), washed with 3% NH₄Cl (2 × 250 mL), 10% NaHCO₃ (1 × 250 mL) and saturated

NaCl (1 × 250 mL), dried (MgSO₄), and evaporated to dryness. The reaction yielded faintly yellow thick oil. The oil was crystallized from EtOAc/Hexane to give shiny rod-like crystals in 80.5% (9.52 g) yield. $[\alpha]_D^{20} = -24.3$ ($c = 1.025$, EtOAc) (lit [1] -24.8 , $c = 1.00$, EtOAc); mp 105-107°C (lit [1] 103.5-105°C); TLC (2:1, EtOAc:Hexane), $R_f = 0.42$; ¹H NMR (CDCl₃, 400 MHz) δ 0.82 (s, 3H), 2.51 (t, 1H), 3.61 (m, 2H), 3.85-3.95 (m, 8H), 5.12 (m, 2H), 5.30 (d, 1H), 7.25-7.39 (m, 5H). High resolution MS calc'd for C₁₆H₂₁NO₆Na (M+Na⁺) 346.12611, found 346.12608 (M+Na⁺).

3.3.4 Cbz-L-Ser(ald)-OBO Ester, 4

[1-(4-Methyl-2,6,7-trioxa-bicyclo[2.2.2]oct-1-yl)-2-oxo-ethyl]-carbamic acid benzyl ester, Cbz-L-Ser(ald)-OBO Ester, **4**. Cbz-L-Ser-OBO Ester, **3**, (9.1 g, 28 mmol) was dissolved in freshly distilled CH₂Cl₂ (80 mL) under Ar and cooled to -78 °C in flask 1 (100 mL RBF). 22.5 mL of oxalyl chloride (2.0 M in DCM, 45 mmol, 1.60 equ) was added to dry CH₂Cl₂ (100 mL) in a separate 250 mL round-bottom flask (flask 2) under Ar and cooled to -78 °C. Dry DMSO (7 mL, 90 mmol, 3.2 equ) was added to the oxalyl chloride solution (flask 2), and the mixture was stirred at -78 °C for 15 min. The solution in flask 1 was transferred slowly by cannula to flask 2 over a period of 45 min and then rinsed with dry CH₂Cl₂ (25 mL). The resulting cloudy, white mixture was stirred for 1.5 h at -78 °C. DIPEA (24.27 mL, 0.14 mol, 5 equ) was added and the solution stirred for 30 min at -78 °C and 10 min at 0 °C. Ice-cold CH₂Cl₂ (250 mL) was added, and the solution was washed

with ice-cold 3% NH_4Cl (3 × 250 mL) aqueous 10% NaHCO_3 (1 × 250 mL) and saturated NaCl (1 × 250 mL), dried (MgSO_4), and evaporated to dryness. The product was placed on hi-vacuum for 24 hours to remove any solvent remaining to ensure dryness. The reaction yielded a pale yellow solid in 91.3% (7.92 g) yield. $[\alpha]_D^{20} = -78.1$ ($c = 0.95$, EtOAc) (lit [1] -99.3 , $c = 1.03$, EtOAc); TLC (1:1, EtOAc:Hexane), $R_f = 0.8$; $^1\text{H NMR}$ (CDCl_3 , 400 MHz) δ 0.81 (s, 3H), 3.82-3.98 (br m, 6H), 4.61 (d, 1H), 5.04-5.16 (br m, 2H), 5.36 (d, 1H), 7.24-7.40 (br m, 5H), 9.69 (s, 1H). High resolution MS calc'd for $\text{C}_{16}\text{H}_{19}\text{NO}_6\text{Na}$ ($\text{M}+\text{Na}^+$) 344.11046, found 344.11051 ($\text{M}+\text{Na}^+$).

3.3.5 Cbz-L-Glu(OtBu)(β -OH)-OBO Ester, 5

4-Benzyloxycarbonylamino-3-hydroxy-4-(4-methyl-2,6,7-trioxa-bicyclo[2.2.2]oct-1-yl)-butyric acid tert-butyl ester, **5**. Zinc powder (100 mesh, 0.500 g, 7.70 mmol, 5 equ), iodine (2 small crystal), and dry THF (30 mL) were heated to reflux in a dry 100-mL flask under Ar. *Tert*-butyl bromoacetate (1.25 mL, 7.70 mmol, 5 equ) was added quickly to the refluxing solution and rinsed with 5 mL THF. Solution was allowed to reflux until all Zn had reacted, approx 15 mins. At that point, a solution of crude Cbz-L-Ser(ald)-OBO Ester, **4**, (0.500 g, 1.17 mmol, assuming 100% yield of the aldehyde from oxidation) in 15 mL of THF was added. The solution was refluxed for 20 min, allowed to cool to room temperature (approximately 30 mins), and then poured into 150 mL of aqueous 5% NH_4Cl . CH_2Cl_2 (100mL) was added, and the organic layer was separated, washed with 5% NH_4Cl (1 × 150 mL) and saturated NaCl (1 × 150 mL), dried (MgSO_4), and

evaporated to dryness yielding clear oil. Purification by flash column chromatography (silica gel, 2:1 EtOAc:hexane), and recrystallization gave 0.320 g (68% yield over two steps) of a white solid. mp 48-51°C (previous unpublished work 48-51°C); $[\alpha]_D^{20} = -6.3$ (c = 1.00, EtOAc) (previous unpublished work $[\alpha]_D^{20} = -6.2$ c = 1.00, EtOAc); TLC (1:1, EtOAc:hexane) $R_f = 0.61$; $^1\text{H NMR}$ (CDCl_3 , 400 MHz) δ 0.82 (s, 3H), 1.43 (m, 9H), 2.38-2.50 (m, 2H), 3.03 (s, 1H), 3.82-3.96 (m, 7H), 4.62 (m, 1H), 5.12 (m, 1H), 5.35 (d, 1H), 7.23-7.38 (m, 5H); High resolution MS calc'd for $\text{C}_{22}\text{H}_{31}\text{NO}_8$ ($\text{M}+\text{H}^+$) 438.21224, found 438.21223 ($\text{M}+\text{H}^+$).

3.3.6 Cbz-L-Glu(OtBu)(β -OH)-OH, **6**

2-Benzyloxycarbonylamino-3-hydroxy-pentanedioic acid 5-tert-butyl ester, Cbz-L-Glu(OtBu)(β -OH)-OH, **6**. Cbz-L-Glu(OtBu)(β -OH)-OBO Ester, **5** (0.15g, 0.34 mmol) was dissolved in 40 mL EtOAc. 4 mL of 5% TFA solution in DCM was added and the reaction mixture was stirred for 2 h under Ar. Conversion to intermediate product 2-Benzyloxycarbonylamino-3-hydroxy-pentanedioic acid 5-tert-butyl ester 1-(3-hydroxy-2-hydroxymethyl-2-methyl-propyl) ester, was checked by MS [calc'd for $\text{C}_{22}\text{H}_{33}\text{O}_9\text{N}$ for 455.50, found 456.26 (MH^+)]. The reaction mixture was evaporated to oil, and re-dissolved in 40 mL THF. 40 mL of LiOH (45mM, 5 equ) was added to the solution, and stirred for 20 h at room temperature. The solution was acidified with 0.1N HCl to pH4.0, and extracted with EtOAc (3 x 50 mL). The organic layer was dried (MgSO_4) and evaporated to an oil. Purification by flash column chromatography (silica gel, EtOAc) and recrystallization (acetone: CH_2Cl_2) yielded colorless crystals (78-96%, 0.96 g -

0.118 g): mp 58-60 °C; $[\alpha]_D^{20} = +1.1$ (c = 0.52, acetone); TLC (acetone) $R_f = 0.25$; $^1\text{H NMR}$ (acetone- d_6 / D_2O , 400 MHz) δ , 1.42 (s, 9H), 2.38-2.60 (br m, 2H), 4.38 (b, 1H), 4.63 (b, 1H), 5.01-5.15 (br m, 2H), 7.22-7.42 (br m, 5H); High resolution MS calc'd for $\text{C}_{17}\text{H}_{23}\text{NO}_7\text{Li}$ ($\text{M}+\text{Li}^+$) 360.16291, found 360.16325 ($\text{M}+\text{Li}^+$).

3.3.6 General Protocol for Cleavage of Protecting Group

32 mL of a 80% TFA/20% H_2O solution was added to a 10 mL of

3.3.7 General Liquid Phase Peptide Coupling and Phosphorylation

1 equ of Cbz-*L*-Glu(OtBu)(β -OH)-OH is dissolved in CH_2Cl_2 :DMF (1:1, 40 mL) along with 0.1 equ HOBt, 0.95 equ HBTU and 1 equ of DIPEA x under nitrogen and stirred for 5 min. 1.2 equ of the C-terminal amine was added to the reaction vessel and stirred for 24 h. Solvent was removed under strong vacuum to produce a yellow mixture of oil and solid. The mixture was brought up in a minimum volume of CH_2Cl_2 and purified by flash column chromatography (silica gel, CH_2Cl_2). Dibenzyl *N,N*-diethylphosphoramidite (12 equ) is added to a solution of the Cbz *N*-protected dipeptide in THF (10 mL) under argon in a 50 mL RBF. 1H-Tetrazole (2.5 equ) is then quickly added to the solution and stirred for 25 min at room temperature. The solution is cooled in an acetone/dry ice bath and a solution of 85% mCPBA (12 equ) in CH_2Cl_2 is slowly added, the solution is removed from the dry ice bath and allowed to stir for 20 min at room temperature. 10 mL of a 10% $\text{Na}_2\text{S}_2\text{O}_5$ solution is added to the mixture and the aqueous phase is separated and discarded. The ethereal phase is washed with 10% $\text{Na}_2\text{S}_2\text{O}_5$ (1 x 30 mL), 5% NaHCO_3 (2 x 30 mL), 5% citric acid (pH 3.3: 1 x 30 mL) and

backwashed with 5% NaHCO₃ (30 mL), dried with MgSO₄ and filtered. Solvent was removed *in vacuo* to produce an oil. The product was lyophilized to remove any trace water, and the phosphorylation process was repeated once more. The product was verified using MS then immediately cleaved.

3.3.8 General Protocol for Cleavage of Protecting Group

50 mL of a 95% TFA/5% H₂O solution was added to a 100 mL RBF containing the protected phospho-dipeptide and stirred for 4 hours. TFA and H₂O were removed *in vacuo* and the resulting product was brought up in 50 mL H₂O and 20 mL Et₂O. The ethereal phase was discarded and the aqueous phase washed with Et₂O (2 x 20 mL). The solvent was removed *in vacuo* to ensure complete removal of any organic solvent, and lyophilized. The product was purified using RP HPLC (solvent A: H₂O, solvent B: Acetonitrile).

3.3.9 Solid Phase Peptide Synthesis

PAL resin (100 mg, 0.05 mmol) was swelled in CH₂Cl₂ (20 mL for 10 min), and rinsed with DMF (2 x 20 mL). For every amino acid coupling cycle, the Fmoc group was removed using 20% piperidine in DMF (20mL for 2x10 min). After washing the reaction vessel carefully with DMF (4 x 20 mL), a solution of amino acid (4 equ), HOBt (3.8 equ), HBTU (0.5 equ), and DIPEA (4 equ) in DMF/DCM (20 mL) was added to the resin, shaken for 4 h washed, rinsed and repeated.

3.3.10 Resin Cleavage and Protecting Group Removal

A solution of TFA/H₂O (95:5) was used to simultaneously cleave the resin- amide bond and remove all protecting groups except the Cbz group. 50 mL of solution was used and stirred for 6 hours. The solution was filtered to remove resin and the solvent was removed *in vacuo*. The resulting product was brought up in 50 mL H₂O and 30 mL Et₂O and the ethereal phase discarded. The aqueous phase was washed with Et₂O (2 x 30 mL). Solvent was removed *in vacuo* to ensure complete removal of any organic solvent and lyophilized. Product was purified using RP HPLC (solvent A: H₂O, solvent B: Acetonitrile). The peptides were then checked by high resolution MS analysis.

Compounds 14 through 17 are categorized by the retention time and MS. Results are summarized in Table 3.1

| Name | HPLC RT (min) (5-95% /90min) | Purity (%) | Mass Spectrometry FTMS Calc'd:obs (ppm) |
|---|------------------------------|------------|---|
| Cbz-L-Glu(β -phos)-morpholine, 14 | 36.86 | 95.3 | 447.11631 : 447.11663 0.7157 ppm |
| Cbz-L-Glu(β -phos)-cyclohexylamine, 15 | 33.16 | 89.7 | 459.15269 : 459.15271 0.0436 ppm |
| Cbz-L-Glu(β -phos)-methylpiperazine, 16 | 18.82 | 96.4 | 460.14794 : 460.14802 0.1739 ppm |
| Cbz-L-Glu(β -phos)-Pip-NH ₂ , 17 | 26.77 | 94.8 | 510.12480 : 510.12483 0.0588 ppm |

Table 3.1 Summary results of peptides synthesized.

3.3.11 Chymotrypsin Coupled Kinetic Assay

Assay buffer contained 50 mM HEPES, 0.1 M NaCl, 5 mM NaN₃ and was brought to pH 7.4 with NaOH (amount used varied to maintain a consistent end volume of 2 mL per assay). Chymotrypsin solution (50 mg/mL in 1 mM HCl, 50 μ L per assay) was made fresh in 500 μ L quantities and stored at 0°C to ensure minimal degradation of chymotrypsin. The Pin1 substrate solution was prepared using dry TFE and contained 25 mM of Suc-AEPF-pNA ($k_{cat}/K_m = 3410 \text{ mM}^{-1} \text{ s}^{-1}$), and 0.3M LiCl. Pin1 solution was prepared at 0.125 mg/mL (50 μ L per assay; 170 nM final concentration)

The assay buffer and substrate solution were added to a clean cuvette and equilibrated until 0°C was reached. When used, Pin1 inhibitors were added directly to the buffer and substrate in the cuvette prior to assay start. Assays were performed at 0°C to minimize proteolytic degradation of Pin1 and chemical conversion of *cis* substrate to *trans*.

Measurement of absorbance was started and chymotrypsin solution was added to the cuvette. When absorbance reached a steady state Pin1 solution was added quickly and reaction was allowed to go to completion. Measurements of the Pin1 constants were performed according to Kofron *et al.* [3] and evaluated by Microsoft Excel.

Chapter Three References

1. Nicholas G. W. Rose, Mark A. Blaskovich, Alex Wong and Gilles A. Lajoie, *Synthesis of enantiomerically enriched b,g-unsaturated- α -amino acids*. Tetrahedron 57 (2001) 1497-1507
2. *Preparation of 1-[N-Benzyloxycarbonyl-(1S)-1-amino-2-oxoethyl]-4-methyl-2,6,7-triosabicyclo[2.2.2]octane*. Organic Syntheses, Coll. Vol. 10, p.73 (2004); Vol. 79, p.216 (2002).
3. Kofron, J.L., et al., *Determination of kinetic constants for peptidyl prolyl cis-trans isomerases by an improved spectrophotometric assay*. Biochemistry, 1991. **30**(25): p. 6127-34.

Chapter Four: Conclusion

4.1 Conclusion

Alterations in the expression levels, in either direction, of human Pin1 can have an effect on the development of cancer and other diseases caused by cell cycle deregulation, Tau related pathologies, as well as HIV proliferation. The phosphorylation dependency that Pin1 exhibits makes it an attractive target for specific anti-cancer and anti-HIV drugs. Unfortunately, reduced Pin1 activity has been shown to increase tau related pathologies such as Alzheimer's disease. Being able to control the rate of Pin1 activity in neural tissue may be valuable in studying Alzheimer's disease.

Slight modifications to the work-up of the Reformatsky addition proved to increase the yield of the reaction from a reported 27% to 68%.

Substituting the proline in Cbz-L-Glu(β -phos)-Pro-NH₂ with pipercolic acid improved the inhibition capabilities from 54.1 \pm 1.8 μ M to 45.4 \pm 1.1 μ M, as determined using full length Pin1 in the chymotrypsin-coupled kinetic assay. Substituting proline with N-methylpiperazine demonstrated stronger inhibition qualities with a K_i of 22.7 \pm 1.4 μ M.

These small inhibitors have advantages over the larger counter parts developed in other research laboratories. While many other inhibitors to date exhibit stronger K_i values, much of these have peptide sequences which, presumably, interact with Pin1 at sites removed from the active site. The smaller,

site-specific di- or tripeptides, which act solely at the active site of Pin1, may diminish nonspecific binding *in vivo*.

In summary, we were able to increase the efficiency of the methods used to stereospecificly synthesize Cbz-L-Glu(t-butyl)(β -hydroxy)-OBO, synthesize novel Pin1 inhibitor candidates, screen them for activity using a chymotrypsin-coupled enzymatic assay, and discover two stronger acting inhibitors over Cbz-L-Glu(β -phos)-Pro-NH₂. Unfortunately, discovery of a nanomolar inhibitor was not achieved.

4.2 Future Work

The work in this thesis furthers the research work from previous theses from this lab. The author suggests that further research be taken to investigate the crystal or possibly the NMR structure of Pin1 bound to the small inhibitor Cbz-L-Glu(β -phos)-Methylpiperazine, **16**, and Cbz-L-Glu(β -phos)-Pip-NH₂, **17**. This would provide structural evidence that the negatively charged glutamic acid does interact with the positively charged Lys63 or Arg68 as postulated. The structural information would also provide details on any contact with the deeper proline binding pocket in which the dual histidines reside. This information could lead to structural based designs of better small inhibitors.

Based on the published structure of the pipecolic acid naphthylalanine containing peptide by Zhang *et al.* this author strongly suggests further work into the synthesis of Cbz-Glu(β -phos)-Pip-NAL-NH₂, possibly through non-solid phase synthesis strategies. The author also suggests that further research into

targeting various kinases and phosphatases, which are known to be active in cancer proliferation, using the optimized methodology and structure of the Pin1 inhibitors demonstrated in this thesis.

1. *Journal of Medicinal Chemistry*, 2012, 55(12), 2107-2116

2. *The University of Queensland*, 2012, 2012-2013

3. *Western Sydney University*, 2012, 2012

4. *Journal of Medicinal Chemistry*, 2012, 55(12), 2107-2116

5. *Journal of Medicinal Chemistry*, 2012, 55(12), 2107-2116

6. *Journal of Medicinal Chemistry*, 2012, 55(12), 2107-2116

7. *Journal of Medicinal Chemistry*, 2012, 55(12), 2107-2116

8. *Journal of Medicinal Chemistry*, 2012, 55(12), 2107-2116

9. *Journal of Medicinal Chemistry*, 2012, 55(12), 2107-2116

10. *Journal of Medicinal Chemistry*, 2012, 55(12), 2107-2116